ELSEVIER

European Journal of Radiology 49 (2004) 143–178

EJR
EUROPEAN JOURNAL OF RADIOLOGY

www.elsevier.com/locate/ejrad

Intracranial pathology of the visual pathway

W. Müller-Forell*

Institute of Neuroradiology, Medical School University of Mainz, Langenbeckstrasse 1, D-55101 Mainz, Germany

Received 4 September 2003; received in revised form 8 September 2003; accepted 9 September 2003

Abstract

Intracranial pathologies involving the visual pathway are manifold. Aligning to anatomy, the most frequent and/or most important extrinsic and intrinsic intracranial lesions are presented. Clinical symptoms and imaging characteristics of lesions of the sellar region are demonstrated in different imaging modalities. The extrinsic lesions mainly consist of pituitary adenomas, meningeomas, craniopharyngeomas and chordomas. In (asymptomatic and symptomatic) aneurysms, different neurological symptoms depend on the location of aneurysms of the circle of Willis. Intrinsic tumors as astrocytoma of any grade, ependymoma and primary CNS-lymphoma require the main pathology in the course of the visual pathway. Vascular and demyelinating diseases complete this overview of intracranial lesions.

Keywords: MRI; Intrinsic; Extrinsic brain lesions; Ischemia; Metastasis; Demyelinating disorders

1. Introduction

In intracranial lesions, ophthalmologic symptoms depend on the site of the lesion affecting visual pathway structures. The most important symptom is loss of visual acuity, whether acute or slowly progressing. Especially the latter with only subtle visual deficits are often underestimated and attributed to aging or stress problems and imaging is performed only when decompensation of the visual system has become apparent, due to space occupying intracranial lesions, which sometimes have already destroyed the surrounding neural substance.

The variety of intracranial lesions affecting any part of the visual pathway is presented according to the anatomic course and do not assume completeness.

The multitude of intracranial lesions is dominated by primary brain tumors, whether they are intrinsic or extrinsic. The main group of intrinsic brain tumors (originating from cells covered by pia) is that of glioma, with three major types: astrocytoma, oligodendroglioma and ependymoma and so-called mixed gliomas that contain two or more different cell types in varying proportion [1]. Application of intravenous (i.v.) contrast material enables the definition of absent or apparent blood-brain-barrier (BBB) disruption.

Treatment and overall prognosis of the histologically frequently benign extrinsic brain tumors (arising from cells outside the pia) are based upon the correct diagnosis. Intracranial metastasis and secondary brain tumors are defined as tumors, involving the CNS and originate from, but are discontinuous with, primary systemic neoplasms.

Imaging of the intracranial portion of the visual pathway is the domain of MR, as it enables a focused examination of the entire visual pathway along its course from the inner aperture of the optic canal to the occipital pole. Its use is mandatory for extrinsic tumors, as the superior contrast resolution and multiplanar imaging capacity enable the identification of anatomic markers as cardinal features of an extraaxial lesion. These include cerebrospinal fluid (CSF) clefts, recognized as crescentic bands, pial blood vessels and/or the dura. The use of i.v. contrast agents enables the demonstration of compartmentalization of extrinsic lesions, since a large number of these tumors show an extensive contrast enhancement (meningeoma, metastasis), while others show none (epidermoid and dermoid tumors) [2].

Metastasis account for up to 30% of all intracranial tumors, the most frequent primary malignancies include lung and breast carcinoma (Fig. 1) [3], hypernephroma, melanoma and neuroblastoma [1]. All areas of the brain may be affected, with preference of the corticomedullary junction as the starting point [1].

* Tel.: +49-6131-17-7139; fax: +49-6131-17-6643.
E-mail address: mueller-forell@neuroradio.klinik.uni-mainz.de (P.D.W. Müller-Forell).

0720-048X/$ – see front matter © 2003 Elsevier Ireland Ltd. All rights reserved.
doi:10.1016/j.ejrad.2003.09.003

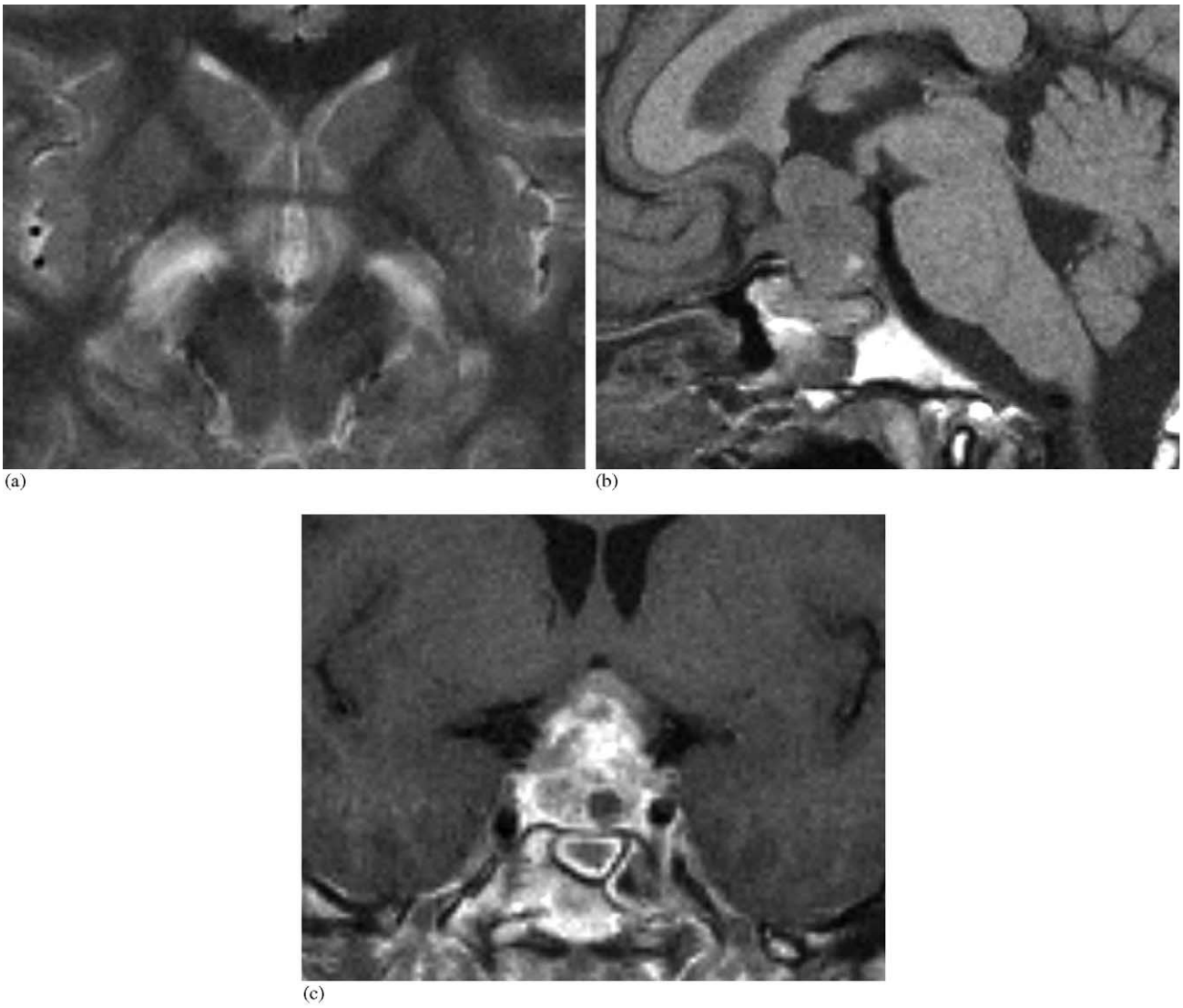

Fig. 1. MR of a 36-year-old female with acute vision loss, predominantly of the right eye, and history of breast carcinoma. Diagnosis: intra- and suprasellar metastasis. (a) Axial T2w view at the level of the anterior commissure show edema along both optic tracts. (b) Midsagittal T1w native view, demonstrating the impression of the floor of the third ventricle, but no identification of the chiasm. (c) Coronal T1w contrast enhanced view, where the chiasm is identified. Note the additional infiltration of the pituitary gland. ((c) With permission of Müller-Forell, 2002.)

2. Sellar region

As already mentioned, in slowly progressing unilateral visual impairment lesions of the chiasmal region are frequently seen at a stage, when decompensation of the visual system has become apparent. In patients suffering from double vision or acute ptosis, the subjective disabling symptoms lead to both an earlier identification of homonymous defects of the visual field and corresponding earlier indication for imaging. Most common causes for bitemporal hemianopia are midline tumors, which cause inferior compression of the chiasm at the crossing site of the nasal fibers.

The chiasm represents the centre of the sellar region, the most complex area of the endocranium, consisting of various tissues, as parenchymal structures, vessels and cranial nerves. As a consequence, a number of more than 30 different pathologic processes, primarily extrinsic lesions may occur, involving and affecting structures of the sellar and juxtasellar region [4]. These mainly benign tumors involve the brain parenchyma secondarily and are often cured completely without recurrences even if they have reached a considerable size. The sellar region is less frequently involved by intrinsic tumors, which often show recurrences, even for benign tumors. Visual disturbances, caused by chiasmal or optic nerve compression, is the most frequent clinical symptom, although these are as variable as the locations of the diseases of the sellar region, ranging from endocrinological disorders (pituitary, hypothalamic insufficiency) and complex focal episodes (temporal lobe), to cranial nerve deficits (cavernous sinus).

2.1. Neoplasms and tumor-like lesions

2.1.1. Extrinsic lesions

2.1.1.1. Pituitary adenoma. Pituitary adenoma, which represent 10–15% of all intracranial tumors, frequently manifest in adults. They are benign, slow growing tumors, composed of cells of the adenohypophysis, normally wrapped up by a pseudocapsule, which enables good demarcation from adjacent structures. In contrast to the group of microadenomas (diameter <10 mm), patients presenting with the characteristic clinical symptom of bitemporal hemianopia, due to inferior compression of the chiasm, harbour endocrinological mainly inactive macroadenoma (diameter

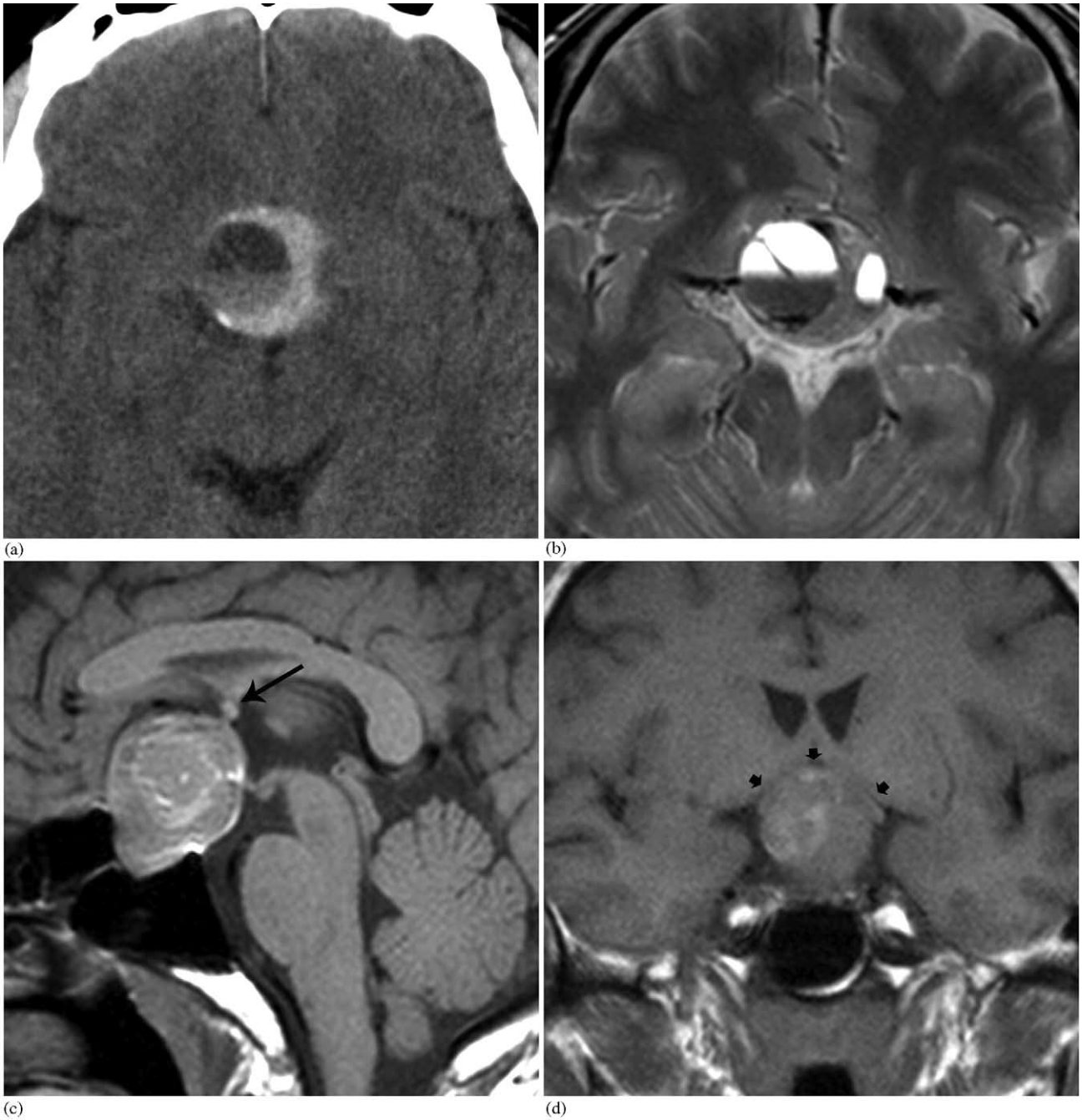

Fig. 2. A 35-year-old male presenting with acute vision loss combined with reduced consciousness and severe headache. Diagnosis: adenoma apoplecticum. (a) Axial native CT, where a suprasellar mass with hyperdense rim is seen. Note the different intensities of a fluid level, representing intratumoral hemorrhage. (b) Corresponding axial T2w image with better delineation of two tumor-cysts. (c) Sagittal T1w view showing the entire tumor extension. Note the dislocation of the chiasm (arrow). (d) Coronal T1w view, demonstrating the inferior impression and cranial dislocation of the chiasm (small arrows), the hazy hyperintensities represent parts of the intratumoral hemorrhage. (e) Corresponding T1w contrast enhanced view.

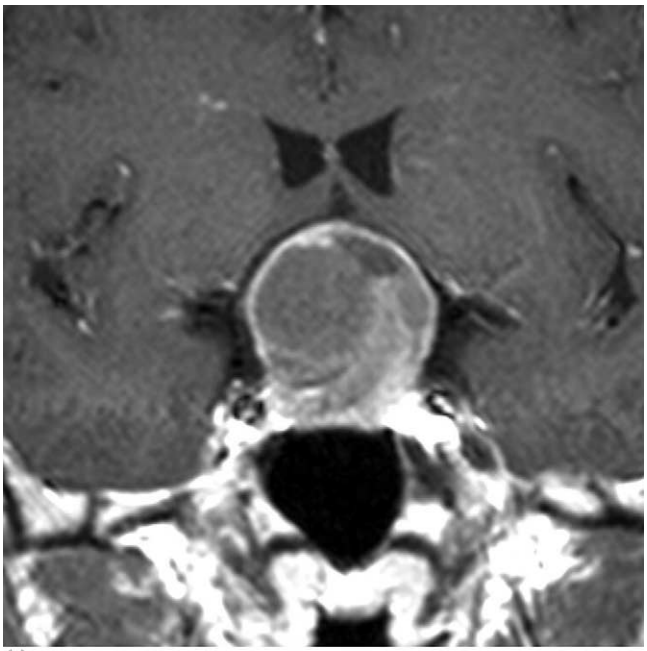

(e)

Fig. 2. (*Continued*).

>10 mm). Acute clinical symptoms of headache, nausea and vomiting are suspicious of an adenoma apoplecticum (Fig. 2). This acute insufficiency of the adenohypophysis is due to a sudden infarction or hemorrhage in the course of tumor growth, but not as frequent as presumed [5].

MR as the method of choice generally shows lengthening of both T1 and T2 relaxation times. The high anatomic resolution and definition of adjacent tissue, i.e. intracranial optic nerves, chiasm and cavernous sinus allow an accurate and conclusive differentiation of the tumor and deformed, compressed and flattened visual structures, especially in native, non contrast enhanced T1w images (Fig. 3). Due to the lack of a solid barrier between the pituitary gland and the cavernous sinus the more reliable indicator for cavernous sinus invasion is the demonstration of a carotid artery encasement or a tumor extension lateral of the cavernous sinus than an even careful analysis of pre- and postcontrast images [5,6]. On T1w non contrast enhanced images, most adenoma show a homogeneous, isointense signal with significant enhancement after contrast application (Figs. 3 and 4). Regressive changes, seen in medium-sized adenomas include cysts and hemorrhages, consequently requiring additional T2w and T2*w sequences (Fig. 2).

Differential diagnosis of pituitary adenoma includes meningeoma of the sellar region (Figs. 4 and 7), craniopharyngeoma (Figs. 9 and 10), optic glioma (Fig. 16), germ cell tumors, chordomas (Fig. 13) and even metastasis (Fig. 1).

A pituitary abscess, mostly caused by gram-positive cocci, is highly uncommon, and clinically presentation is dominated by headache and visual loss. It is known to occur in the presence of sellar mass or by contiguous spread from an infected sphenoid or cavernous sinus [5]. Post contrast imaging demonstrates a rim enhancement around a hypointense centre, representing the necrosis, and additional infiltration of the adjacent sinus and intracranial structures (Fig. 5).

2.1.1.2. Meningeomas. Meningeomas constitute up to 26% of primary intracranial tumors, occurring predominantly, but not exclusively (Fig. 6) in middle-aged and elderly patients with a female dominance [7]. Approximately 20% of meningeomas are located in the sellar region, with 50% arising from midline structures, such as the sphenoid plane (Fig. 6), the tuberculum sella (Fig. 7), diapghragma sella, or the dura of the cavernous sinus. The remaining other 50% consist of sphenoid wing meningeomas or meningeomas of the clinoid process (Figs. 4 and 8). Because of their early alteration of the optic nerve with resulting early ophthalmological problems, globular meningeoma of the suprasellär or paraclinoid region may not exceed 2 cm in diameter [8] (Fig. 8).

Imaging characteristics of meningeoma consist of an isodense/isointense presentation on non-contrast enhanced images, due to their high cell density. Due to high tumor vascularisation and absence of BBB, meningeoma present a homogeneous, intensive enhancement after i.v.-contrast administration, making its indication mandatory in order to detect even tumors or tumor parts in areas only millimetres in size (Fig. 8). MR enables an accurate, detailed description of anatomic and pathologic morphology, especially in question of infiltration of the cavernous sinus and encasement of the internal carotid artery (ICA). Differential diagnosis for globular meningeoma in contrast to giant aneurysms of the ICA is facilitated by the high sensitivity of MR for flow and thrombi; other important lesions to be excluded include supra- and extrasellar pituitary adenoma, trigeminal schwannoma, metastasis and inflammatory granuloma.

2.1.1.3. Craniopharyngeoma. Craniopharyngeoma are defined as benigne, partly cystic, epithelial tumors of the sellar region, corresponding to WHO grade I. They typically show no sex bias but a bimodal age distribution with one peak involving children and adolescents, and the other adults [9]. These tumors, which are assumed to derive from Rathke's pouch epithelium, account for up to 4.6% of all intracranial tumors and represent the second most frequent tumors of the sellar region after pituitary adenomas. Craniopharyngeomas, which can be divided into an adamantinous and a papillary type, often show calcification and cysts (Fig. 9), filled with a thick, cholesterol-rich, brownish-yellow fluid. Adamantinous craniopharyngeoma are more frequently seen in children, while papillary craniopharyngeoma with more solid structures are found more frequently in adults (Fig. 10) [10,11]. Endocrinological deficiencies (diabetes, dwarfism, delayed puberty) are leading clinical symptoms, predominantly in children, while visual disturbances, due to compression of the visual structures are more frequently seen in adults, combined with headache (Fig. 10), nausea, vomiting, and papilledema, the latter as a

Fig. 3. A 39-year-old male with acute visual deficit (blurred vision) and high prolactin level. Diagnosis: pituitary adenoma (prolactinoma). (a) Midsagittal T1w native view, demonstrating the apical dislocation of the chiasm. The arrow indicates the chiasmatic recess of the still acute angled third ventricle. (b) Coronal T1w native view. Note the dislocation of the pituitary stalk to the left (arrow). (c) Corresponding contrast enhanced view, where the small residual adenohypophysis can be delineated (arrows) with bright contrast enhancement.

result of increased intracranial pressure, due to obstruction of the interventricular foramen in quite large lesions [5,11]. CT is still justified for differential diagnosis in view of the characteristic calcification of parts of the tumor, but MR is mandatory for preoperative planning. MR pattern show a great variety: adamantinous craniopharyngeoma primarily shows a combination of T1w hypointense and T2w highly hyperintense signals, whereas in papillary craniopharyngeoma hyperintense signal on T1w and hypointensities on T2w images may dominate [11]. Both tumor types generally show a hyperintense signal of the solid tumor parts with a prominent enhancement of the tumor and the cyst wall [5]. Differential diagnosis include cystic pituitary adenomas, gliomas of the chiasm or hypothalamus, Rathke's pouch cyst, epidermoid, dermoid, germinoma of the third ventricle and suprasellar meningeomas [8,12].

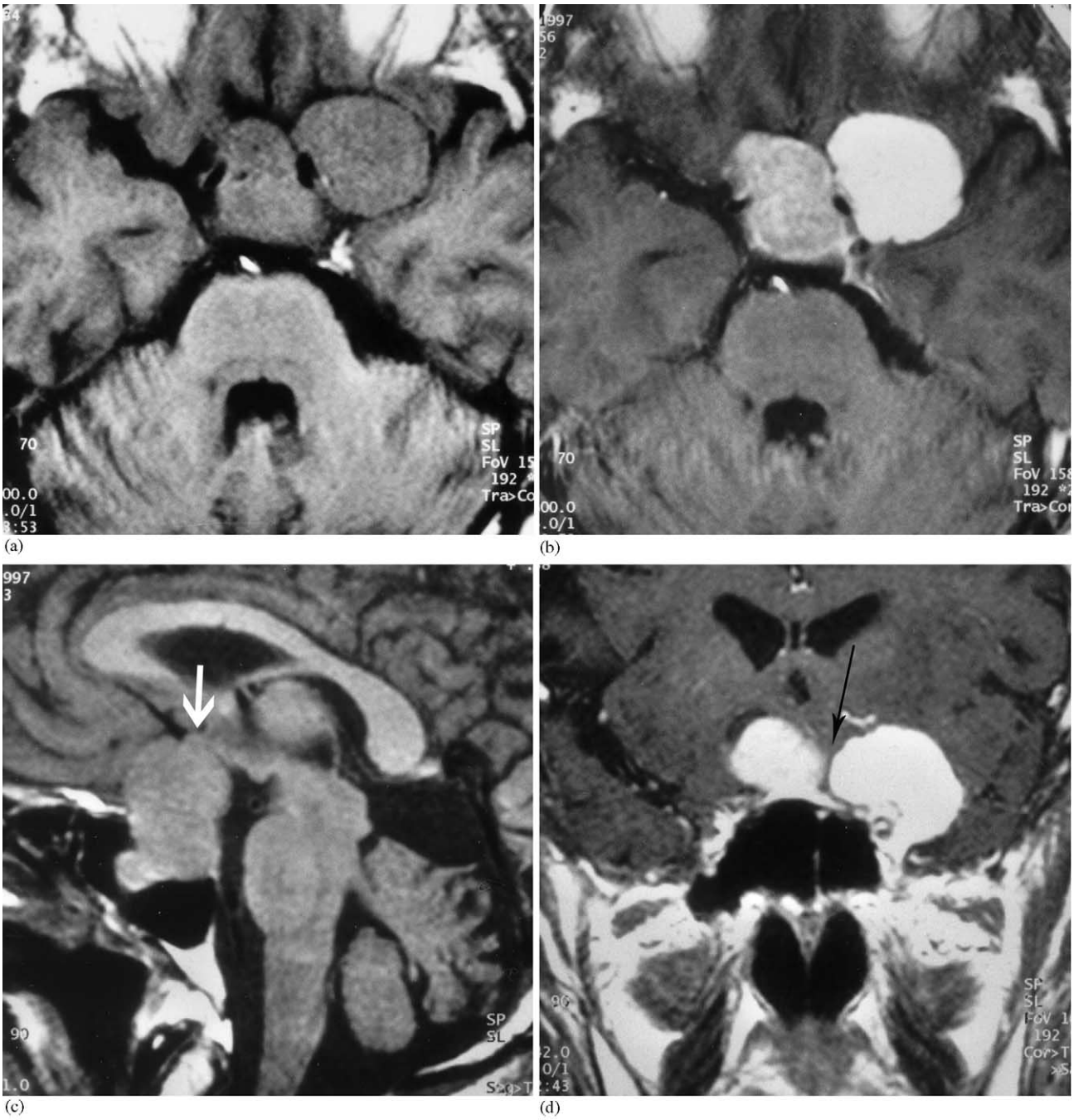

Fig. 4. MR (T1w) of a 73-year-old male presenting with slowly progressing consecutive bilateral blindness of 95%. Diagnosis: pituitary adenoma and additional left sphenoid wing meningeoma. (a) Axial native view presenting isointense signal of both, the median and paramedian space occupying lesions. (b) Corresponding contrast enhanced view, where homogeneous, but different signal enhancement is seen: the adenoma present only with slight, the meningeoma with intense enhancement, leading to diagnosis. (c) Paramedian sagittal native view showing the cranio-caudal extension of the pituitary adenoma, with impression and dislocating of the chiasm (arrow). (d) Coronal contrast enhanced view demonstrating the different tumors by some interposed, extrinsic compressed frontal brain parenchyma. ((a, b) With permission of Müller-Forell, 2002.)

2.1.1.4. Aneurysms. The rupture of an intracranial aneurysm, mainly located at the circle of Willis, is the most common atraumatic cause of subarachnoid hemorrhage (SAH), presenting with a sudden onset of severe headache, varying loss of consciousness, seizure, vomiting and focal neurological deficits, requiring immediate, either neurosurgical or interventional neuroradiological therapy, especially in view of a high incidence of often life-threatening rebleeding. The underlying pathological process of intracranial aneurysms has been recognized as an endothelial dysfunction [13]. Clinical symptoms with visual deficiencies of symptomatic unruptured intracranial aneurysms of the in-

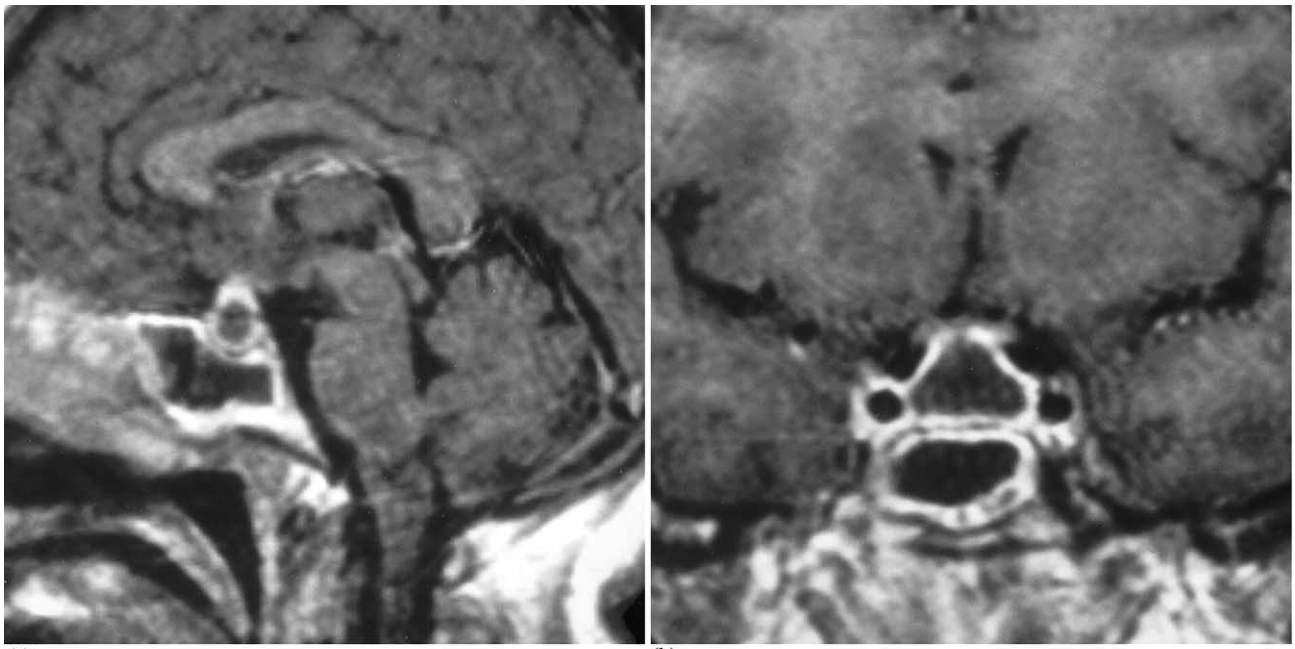

Fig. 5. MR of a 47-year-old female who presented in pituitary coma; after substitution, she complained of headache, variable visual deficits and clinical constellation of meningism and fever. Diagnosis: pituitary abscess. (a) Sagittal T1w contrast enhanced view with ring shaped enhancement of the pituitary and sphenoid sinus. (b) Coronal T1w contrast enhanced view demonstrates complete necrosis of the pituitary gland.

fraclinoid or supraclinoid internal carotid artery (ICA), the anterior cerebral artery (ACA), or the basilar artery depend on the site of compression of visual pathway structures. (Figs. 11–13). Neither the extent nor the clinical symptomatology of slowly progressing visual field deficits caused by aneurysm may be readily distinguished from those caused by tumors. Orbital pain, periorbital or facial pain is the most common symptom of cavernous carotid aneurysms, followed by different types of cranial nerve palsies. Isolated N III palsy may lead to diagnosis of an aneurysm of the posterior communicating artery, while an aneurysm of the ICA is suspected in the presence of a combination of NVI or N IV palsy and a sensory deficit of the trigeminal nerve [14].

In acute subarachnoid hemorrhage CT is the method of choice, as it demonstrates not only the extent of the bleeding itself, but also the volume and distribution of the acute hemorrhage and its complication as acute CSF disturbance. In unruptured aneurysm CT might demonstrate secondary changes as bony erosion of the sphenoid, or calcification of the wall, as these aneurysms are generally larger than ruptured aneurysms. MR is the method of choice in visualizing the vicinity of unruptured aneurysm and their relation to the optic nerve, chiasm or optic tract, due to its multiplanar capability in combination with its high sensitivity and spatial resolution, enabling the detection of flowing blood. Combination of MR images with 3D-TOF (time-of-flight) or 3D phase contrast MRA, enables a detection rate of aneurysms >3 mm in diameter of ≈100% [15]. Intra-arterial DSA of the cerebral vessels still remains the gold standard in the detection or exclusion of intracranial aneurysms as it represents not only the most sensitive method, but enables precise planning and performance of interventional therapy with coil occlusion, preferably using 3D-DSA [16,17].

2.1.2. *Miscellaneous*

Germ cell tumors of the CNS constitute a unique class of rare tumors of different malignant character, affecting children and young adults, but represent only 0.5% of all intracranial neoplasms. About 80% impinge on the midline with preference to the pineal gland, but intra- or suprasellar locations may be involved (Fig. 14), simultaneously or sequentially, if the tumor is multifocal [18]. Hormonal disturbances, due to hypothalamic infiltration may be additional to visual pathway disturbances, as Parinaud syndrome in case of involvement of the quadrigeminal plate, or visual loss and/or cranial nerve palsies in case of suprasellar growth with impingement of the chiasm. On imaging germ cell tumors appear as a solid, homogeneous mass, rarely including cysts, a feature that is in contrast to craniopharyngeoma. In noncontrast enhanced images, they demonstrate an even unspecific character on methods, CT and MR, but show a marked, mainly homogeneous enhancement after administration of i.v. contrast material [4,5].

Chordomas are extremely rare, slow growing, osteodestructive, histologically benign, midline tumors, participating in ophthalmologic disorders only in case of extension towards the chiasm (Fig. 15). Differential diagnosis of these lesions, presenting on imaging with intermediate signal on both T1w and T2w images with moderate contrast enhancement, should include chondromas, chondrosarcomas, metastasis, as well as hormone-inactive pituitary adenomas or even skull base meningeomas [19].

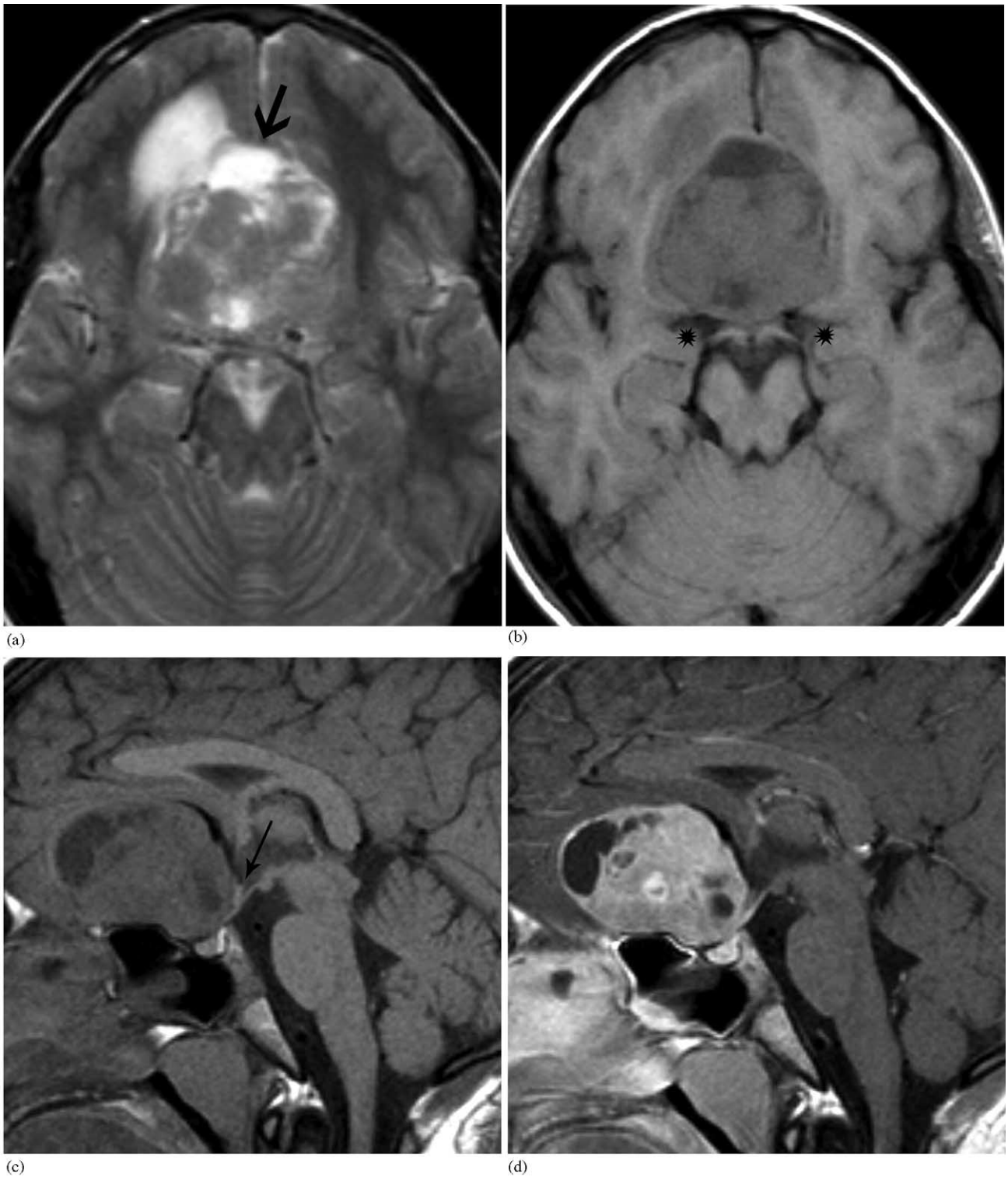

Fig. 6. MR of a 13-year-old boy with quick vision loss on both eyes (1/40 and 1/20). Diagnosis: meningeoma of the sphenoid plane. (a) Axial T2w view, demonstrating a mass in the anterior cranial fossa bilaterally, with lateralization to the right, and with inhomogeneous signal, apparently including a cystic tumor part (arrow). (b) Corresponding T1w native view, where the extrinsic nature of the lesion is seen, as it impresses both frontal lobes. Note the posterior dislocation of the chiasm and both optic tracts (stars). (c) In the T1w native midsagittal view the dislocation of the chiasm is apparent (arrow). (d) Corresponding contrast enhanced view.

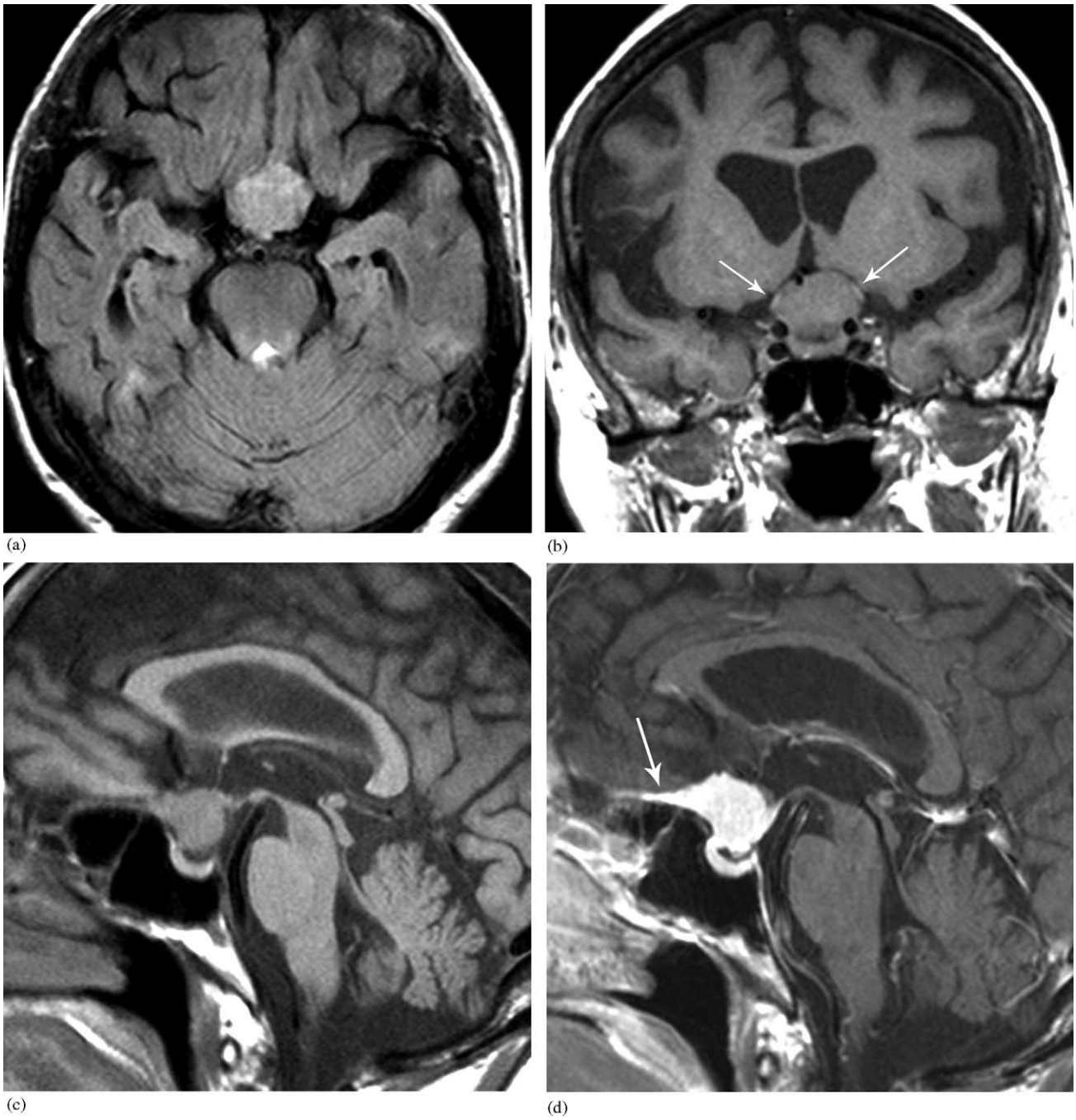

Fig. 7. MR of a 72-year-old female with history of multiple brain infarctions, responsive for variable neurological deficits, who developed a slowly progressing visual deficit with acute deterioration. Diagnosis: meningeoma of the tuberculum sella. (a) Axial T2w FLAIR image with isointens, well delineated suprasellar mass. Note the additional brain atrophy and temporal signal intensities, as residuum of the brain infarctions. (b) Coronal T1w native view with inferior compression of the chiasm (arrows). Note the delineation of the unaffected pituitary gland. (c) Midsagittal T1w native view, demonstrating the globular shape of the meningeoma, located at the sellar tuberculum, and distinct from the pituitary gland. Note the megadolicho configuration of the basilar artery, elevating the floor of the third ventricle. (d) Corresponding contrast enhanced view, where the tumor extension along the sphenoid plane is apparent (so-called 'tumor-tail') (arrow).

2.1.3. Intrinsic lesions

2.1.3.1. Glioma of the chiasm. Gliomas of the anterior visual pathway are uncommon lesions, histologically mainly defined as pilocytic astrocytoma, and mainly affecting children and young adults (see chapter optic nerve). Although most of these gliomas are located in the optic nerve, some show an additional involvement of the chiasm, only 7% of pilocytic astrocytoma demonstrate an exclusive involvement of the chiasm, and 46% touch the chiasm and

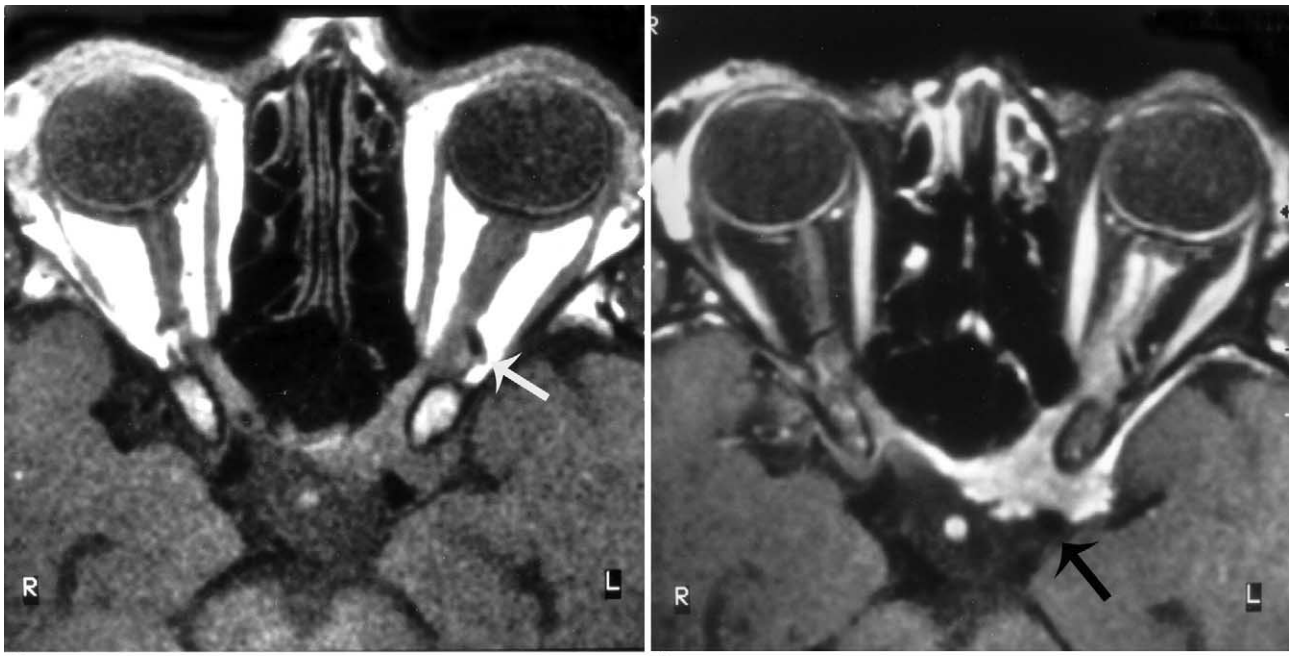

(a) (b)

Fig. 8. T1w MR of a 33-year-old female with known amaurosis of the left eye persisting for two years. Acute presentation with complain of double vision for the previous 2 weeks. Diagnosis: sphenoid wing meningeoma with secondary infiltration of the optic nerve sheath and cavernous sinus. (a) Axial native view with isointense small mass in the area of the left clinoid process, no definite identification of the left optic nerve. Note the slight widening of the left ophthalmic artery (white arrow), compared to the right. (b) Corresponding contrast enhanced (FS) view. Although the intracranial tumor part is small, an extent growth en plaque around the left clinoid process into the ipsilateral and towards the contralateral optic canal with involvement of the left optic sheath is apparent. (With permission of Müller-Forell, 2002.)

hypothalamus (Fig. 16). In cases of an additional or primarily hypothalamic involvement the mortality rate increases to over 50%, since no specific therapy alters the final outcome [20].

Only 10% of gliomas of the chiasm occur in patients older than 20 years [21], representing a clinical entity distinct from the benign gliomas of childhood, due to the fact that they are not associated with NF1 but include malignant astrocytoma or glioblastoma (Fig. 17) and uniformly show a fatal course of usually <1 year [20,22]. Visual impairment of these patients depends on the size and location of the mass.

2.1.3.2. Astrocytoma. Astrocytoma represent the most frequent entity of primary brain tumors with up to 60% of all intracranial neoplasms. They arise from differentiated, neoplastically transformed astrocytes, comprise a wide range of age and gender distribution, growth potential, extent of invasiveness, morphological features, tendency for progression and clinical course [1,23]. Astrocytomas include pilocytic and subependymal giant cell (both WHO I), diffuse low grade astrocytoma (WHO II), anaplastic astrocytoma (WHO III) and glioblastoma (WHO IV). These different entities reflect the type and sequence of genetic alterations acquired during the process of transformation, where the progression from low grade to anapalastic astrocytoma and glioblastoma is associated with the cumulative acquisition of multiple genetic alterations [23]. All astrocytoma are characterized by more or less localized or diffuse infiltration of the adjacent or distant brain parenchyma and may have an inherent tendency for malignant progression, with glioblastoma as the most malignant phenotypic endpoint [23,24].

Pilocytic astrocytoma are more circumscribed intrinsic lesions, which typically present in the fist two decades, with preference to the optic nerve and chiasm and/or hypothalamus (Fig. 18), sometimes associated with clinical diagnosis of NF1 [25]. Diffuse astrocytoma (WHO II), characterized by diffuse infiltration of the adjacent parenchyma with a tendency to malignant progression to anaplastic astrocytoma and, ultimately glioblastoma mainly affect adults. Glioblastoma, representing the most frequent malignant intracranial tumor, account for $\approx 60\%$ of all astrocytoma. The histopathological features are characterized by cellular polymorphism, nuclear atypia, brisk mitotic activity, thrombosis, microvascular proliferation, and necrosis [24]. Imaging features of astrocytoma are as variable as the histopathological ones: low-grade astrocytoma present as mildly hypointense on T1w and hyperintense on T2w images, mainly without any contrast enhancement. BBB disruption may be a factor in tumor progression, and can be assumed in glioblastoma, where the simultaneous delineation of tumor necrotic cysts, sometimes associated with hemorrhages and solid, enhancing tumors parts, combined with reactive brain edema reflects histopathology [24].

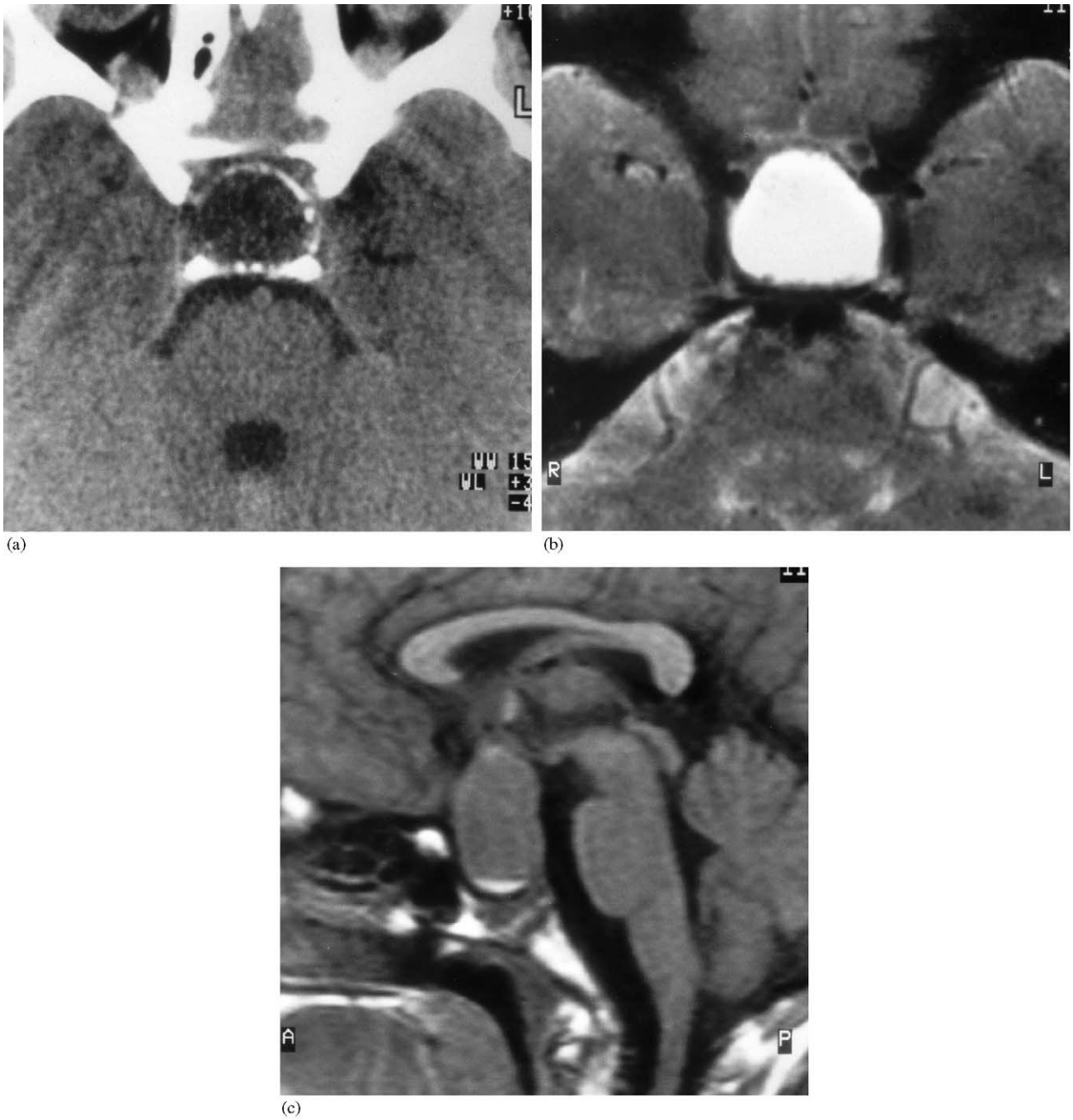

(a) (b) (c)

Fig. 9. A 3-year-old boy with recurrent headache, leading to imaging, but no neuro-ophthalmologic deficit. Diagnosis: craniopharyngeoma. (a) Axial CT with a cystic mass with calcified capsule in a widened sella. (b) Corresponding T2w view, confirming the cystic nature of the mass. (c) Midsagittal T1w native view, presenting the entire cranio-caudal extension of the mass, which demonstrated homogeneous contrast enhancement (not shown).

2.1.3.3. Cavernoma. Calcification can be seen in cavernoma, the only true venous malformation of the CNS, which consists of widened endothelial-lined sinusoidal vascular spaces without any interposed neural tissue. Cavernoma can be found anywhere in the cerebral or spinal tissues, sometimes multifocal. Intralesional hemorrhages are consistently found at pathology, but only few patients present with clinical symptoms of an acute bleeding episode, which is more frequent in cavernoma <10 mm in size. CT may identify intralesional calcification, but specific diagnosis is to be made with MR. Due to the high susceptibility of hemosiderin, especially T2*-weighted sequences demonstrate intralesional or occult hemorrhages/calcification (Fig. 19), not only adjacent to the lesion itself, but also in other regions of the CNS [8,26,27].

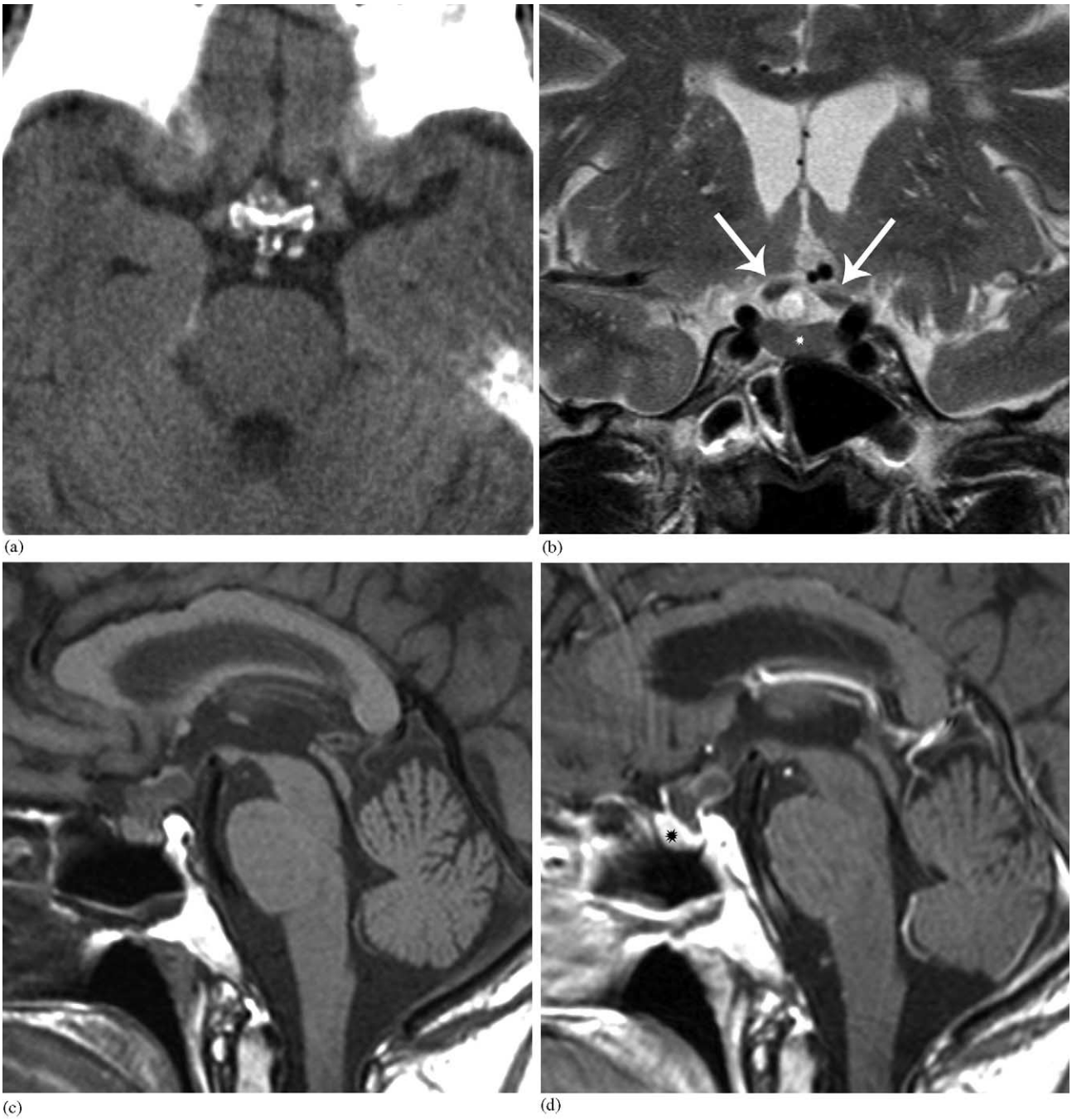

Fig. 10. A 63-year-old female presenting with unspecific visual deficits and beginning right optic nerve atrophy. Diagnosis: craniopharyngeoma. (a) Axial CT, where only slight perisellar calcification were seen. (b) Coronal T2w view, demonstrating a cystic infraoptic lesion at the right. The arrows indicate the lateral parts of the impressed chiasm, the small star the unaffected pituitary gland. (c) Midsagittal T1w native view that shows the only slight inferior impression of the chiasm. Note the impression of the floor of the third ventricle due to megadolicho-basilar artery. (d) Corresponding contrast enhanced view, where the intrasellar expansion of the tumor is apparent. The star marks the unaffected pituitary gland.

3. Optic tract and area

Patients suffering from lesions of the optic tract and visual area present with homonymous hemianopia to the contralateral visual field, but may demonstrate different extent, depending on the kind and location of the underlying pathology (see also chapters of anatomy and neuroophthalmology).

3.1. Neoplasms

3.1.1. Ependymoma

Ependymoma (Fig. 20) are slowly growing intrinsic tumors (WHO grade II), arising from ependymal layers of the ventricles with variable morphologic features and include subependymoma, myxopapillary ependymoma (both WHO

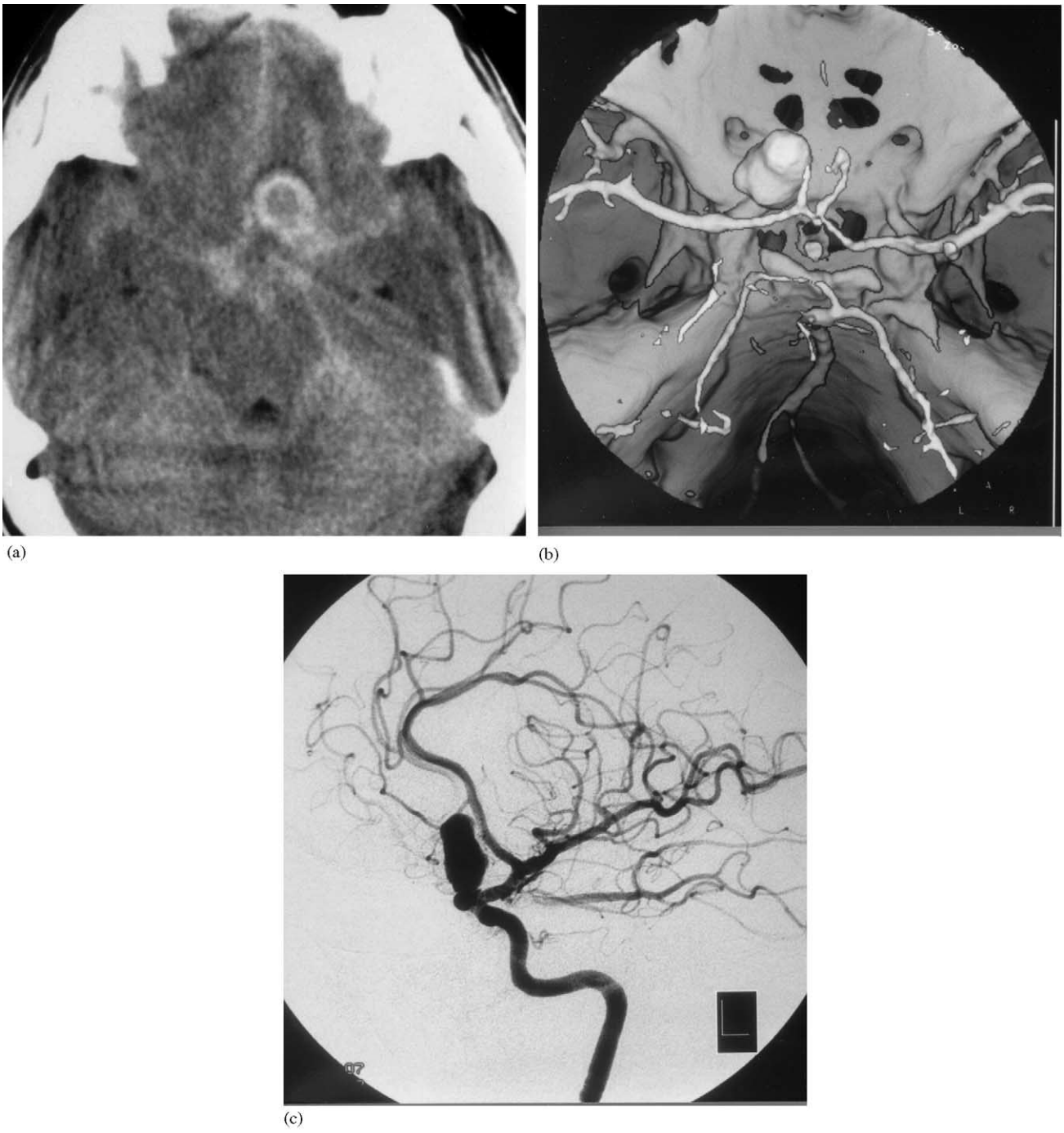

Fig. 11. A 48-year-old woman with acute loss of vision in the left eye, accompanied by severe headache. Diagnosis: acute subarachnoid hemorrhage (SAH) caused by an ophthalmic aneurysm of the left ICA. (a) Axial CT with acute subarachnoid hemorrhage of the basal cisterns and a circular target-shaped formation in the left subcallosal area. (b) 3D-CT-angiography (left is right and vice verse) showing a lobulated aneurysm of the left ICA. (c) DSA of the left ICA in an oblique view to the right, revealing an upwardly directed, slightly lobulated aneurysm of the C5-part of the left ICA. (With permission of Müller-Forell, 2002.)

I), and anaplastic ependymoma (WHO III) (Fig. 21). They account for up to 9% of all neuroepithelial tumors at any site of the ventricular system, preferentially affecting children and young adults, most commonly in the infratentorial compartment (fourth ventricle). In cases of involvement of the supratentorial parenchyma (Fig. 21), again mainly in children and young adults, they originate from embryonic ependymal remnants [28]. On imaging these quite distinctly circumscribed lesions present with heterogeneous signal intensities, low on T2w and slightly hyperintense on T1w imaging, reflecting partly cystic, partly calcified, necrotic and hemorrhagic areas of the mass, while solid tumor parts

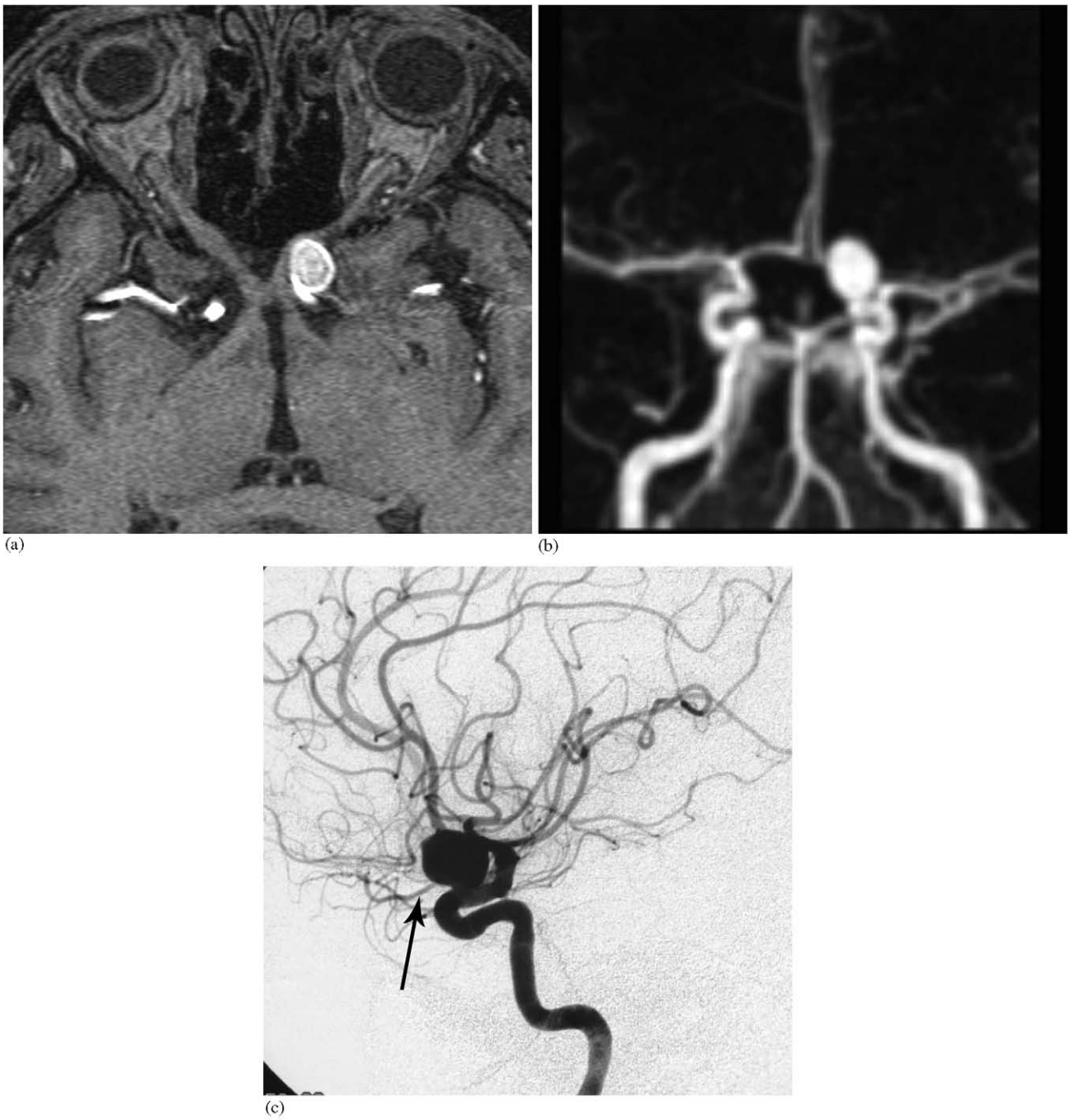

Fig. 12. A 49-year-old woman with chronic headache, leading to imaging, no visual deficits, but signs of left optic nerve compression upon Goldman visual field examination. Diagnosis: incidental ophthalmic aneurysm of the left ICA. (a) Axial T1w high-resolution view (flash 3D), where an impression of the left optic nerve at its proximal intracranial course due to an anteriorly arising aneurysm at the origin of the ophthalmic artery is seen. (b) MR-angiography (MIP reconstruction), demonstrating the superior extension of the lesion. (c) DSA of the left ICA (lateral view) shows the origin of the aneurysm at the origin of the ophthalmic artery (arrow). ((c) With permission of Müller-Forell, 2002.)

show BBB disruption (Fig. 21). MR is the method of choice for detection of additional CSF dissemination, usually found in conjunction with recurrence at the primary site [29].

3.1.2. Primary CNS lymphoma

Primary CNS-lymphoma is defined as extranodal malignant lymphoma arising in the CNS (according to intrinsic lesion) in the absence of obvious lymphoma outside the nervous system at the time of diagnosis (Figs. 22 and 23) and should be differentiated from secondary manifestation of systemic lymphoma (Fig. 24) [30]. In immunocompetent patients, the sixth to seventh decade is the mean age of manifestation, whereas the median age of incidence in immunocomprised patients (organ transplant recipients, con-

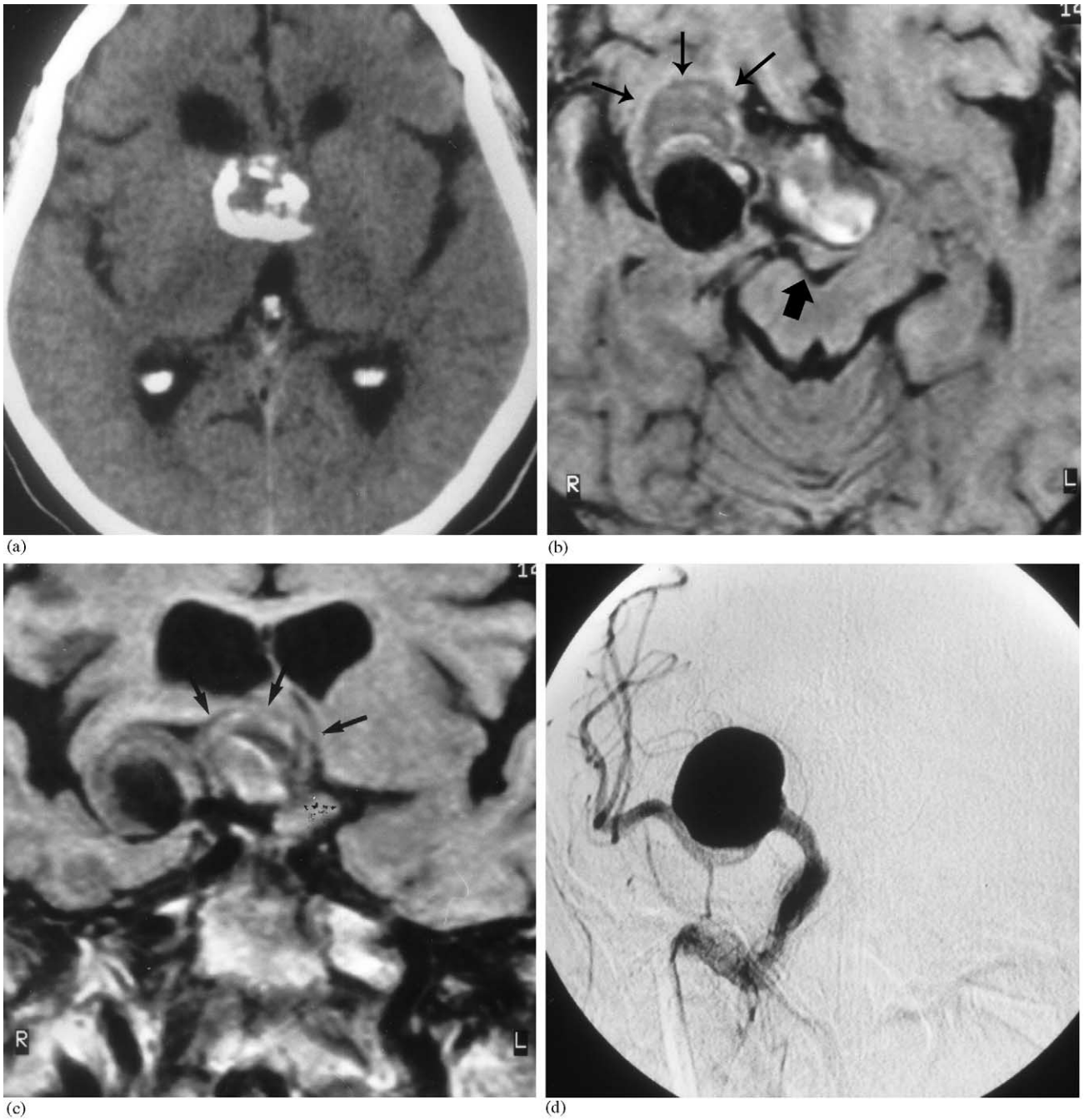

Fig. 13. A 66-year-old woman with pressure sensation behind the right eye and slowly progressing visual deficit, presenting with incomplete N III-paresis of the right eye. Diagnosis: partly thrombosed (butterfly-shaped) aneurysm of the right ICA bifurcation. (a) Axial CT of the suprasellar region with ring-shaped calcification in thee right paramedian region of the basal ganglia and thalamus. (b) Axial T1w native MR of the region of the interpeduncular cistern, demonstrating a flow void of the open aneurysm, in addition to an onion-shaped (older) thrombosed part (small arrows) frontal to the aneurysm. Note the compressed chiasm (big arrow). (c) Coronal T1w native MR documenting the butterfly-shape of the lesion. Note again the flow void of the open part of the aneurysm and the onion-shaped thrombosed area (small arrows) with impression of the basal ganglia. (d) ap View of the DSA of the right ICA, demonstrating the entire open area as well as the origin of the aneurysm at the ICA bifurcation with location of the right M1-segment below. Note the lack of opacification of the ispilateral ACA, which may be due to both compression (by the thrombosed part) and minor antegrade flow. (With permission of Müller-Forell, 2002.)

Fig. 14. MR of an 11-year-old girl with universal infantilism but no visual symptoms. Diagnosis: pituitary and hypothalamic germinoma. (a) Midsagittal T1w native view with enlargement of the optic chiasm and pituitary stalk. (b) Corresponding contrast enhanced view with inhomogeneous signal enhancement of the chiasm, hypothalamus, and pituitary gland. (c) Axial T1w, contrast enhanced view with tumor enhancement of the chiasm and thickened pituitary stalk). (With permission of Müller-Forell, 2002.)

genitally immunodeficient or HIV-patients) ranges from 10 to 39 years [30]. Although the most common location is supratentorial, involvement of the occipital lobe is seen in only 3%. As an exquisite sensitivity to steroids exists, these drugs should be withheld until tissue is obtained for diagnosis by stereotactic biopsy [30,31].

On imaging, classic findings show multiple, sometimes solitary masses involving deep gray matter structures, the corpus callosum, and periventricular regions with moderate perifocal edema (Fig. 22). Slightly hyperdense on CT and isointense on all MR sequences lymphoma present with diffuse to homogeneous contrast enhancement. In case of enhancement along perivascular leptomeningeal spaces (Fig. 23), CNS lymphoma should be put on top of the differential diagnosis, together with sarcoidosis and toxoplasmosis.

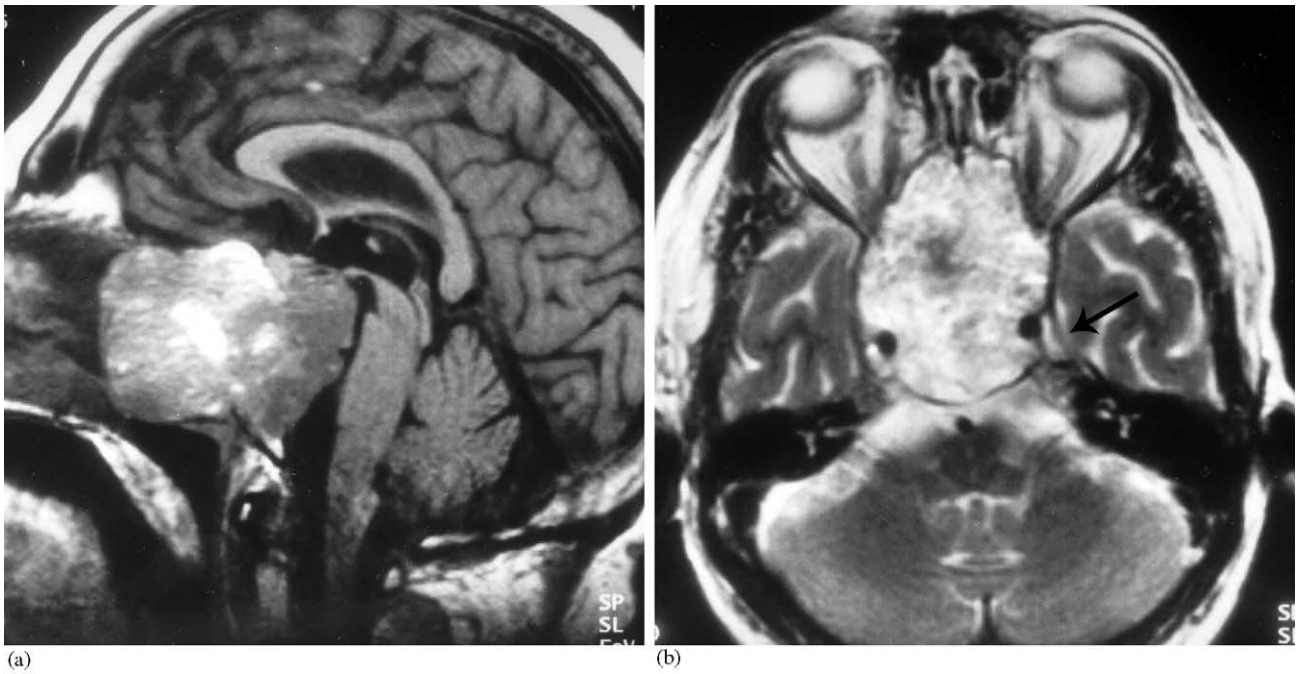

Fig. 15. MR of a 61-year-old woman with slowly progressing visual deficit (only shadow vision) of the right eye. Diagnosis: chordoma. (a) Midsagittal T1w native view, demonstrating the entire tumor growth with complete destruction of the clivus and hard plate, as well as compression of the brainstem, and slight impression of the chiasm. The different signal intensities are due to small intratumoral hemorrhages. (b) Axial T2w view, where the bilateral destruction of the optic canal is demonstrated. The arrow indicates the dislocated left Gasserian ganglion. (With permission of Müller-Forell, 2002.)

3.1.3. Miscellaneous

Meningeomas may arise at any region of the skull, because of their slow growth neurologic symptoms may arise late in respect to tumor size (Fig. 25).

It is the nature of metastasis to mimic many of the primary CNS tumors, and especially in case of up to now unknown primary tumor, when neurologic symptoms indicate imaging, only histology may lead to the right diagnosis (Fig. 26).

3.2. Nonneoplastic lesions

3.2.1. Vascular lesions

Underlying pathology of acute functional disorders of the brain, clinically presenting as stroke, includes a heterogeneous group of cerebrovascular disorders. The four major groups are cerebral infarction (80%) caused by arterial vessel occlusion or as a result of inflammatory vascular disease, spontaneous subarachnoid (5%) or intracerebral hemorrhage (15%) and venous occlusion [32].

The main arterial supply of the optic tract and radiation arises from the territory of the posterior cerebral artery (PCA), which gives rise to the medial and posterior choroidal arteries, which are in hemodynamic balance with the anterior choroidal arteries, arising from the ICA and applying the optic tract. Although considerable variation exists, the PCA mainly supplies the inferior temporal and the occipital lobe [33]. In acute cerebral ischemia and infarction the blood flow is significantly diminished, but the damage to the affected brain depends on vulnerability of the brain, collateral supply, degree and duration of the cerebral ischemia [12].

Imaging is able to reflect the alterations of cell membrane function and loss of cytoskeletal integrity with subsequent cell death in the course of cerebral infarction [32]. In particular MR studies, including T2w, diffusion weighted (DWI) and MRA (MR-angiography) sequences identify the localization of the occlusion and also the area of brain damage earlier and more sensitively than with CT [34]. The acute accumulation of intra- and extracellular edema induces a prolongation of both T1 and T2, resulting in a high signal on T2w images, not always apparent in early scan, where, on the other hand indirect signs (also known on CT) of subtle swelling of the affected gyri and compression of the adjacent sulci should be noted. The most sensitive sequence used in early infarction is diffusion weighted imaging (DWI), including ADC-maps (Fig. 27), as the early cytotoxic edema restricts the water diffusion (restricted Brown's molecular movement), resulting in high signal intensity of infracted brain compared to unaffected normal brain (Fig. 28).

Especially in younger patients, where degenerative arterial lesions are unlikely vasculitis should be taken into differential diagnosis consideration. Vasculitis is defined by its pathological findings of inflammation and necrosis of the blood vessel wall, with involvement of virtually any size or type of organ system [35]. In general CNS involvement is rather uncommon, and isolated CNS vasculitis rather rare [36], but classification of CNS vasculitis vary from primary (e.g. periarteritis nodosa, giant cell arteritis, Wegener's

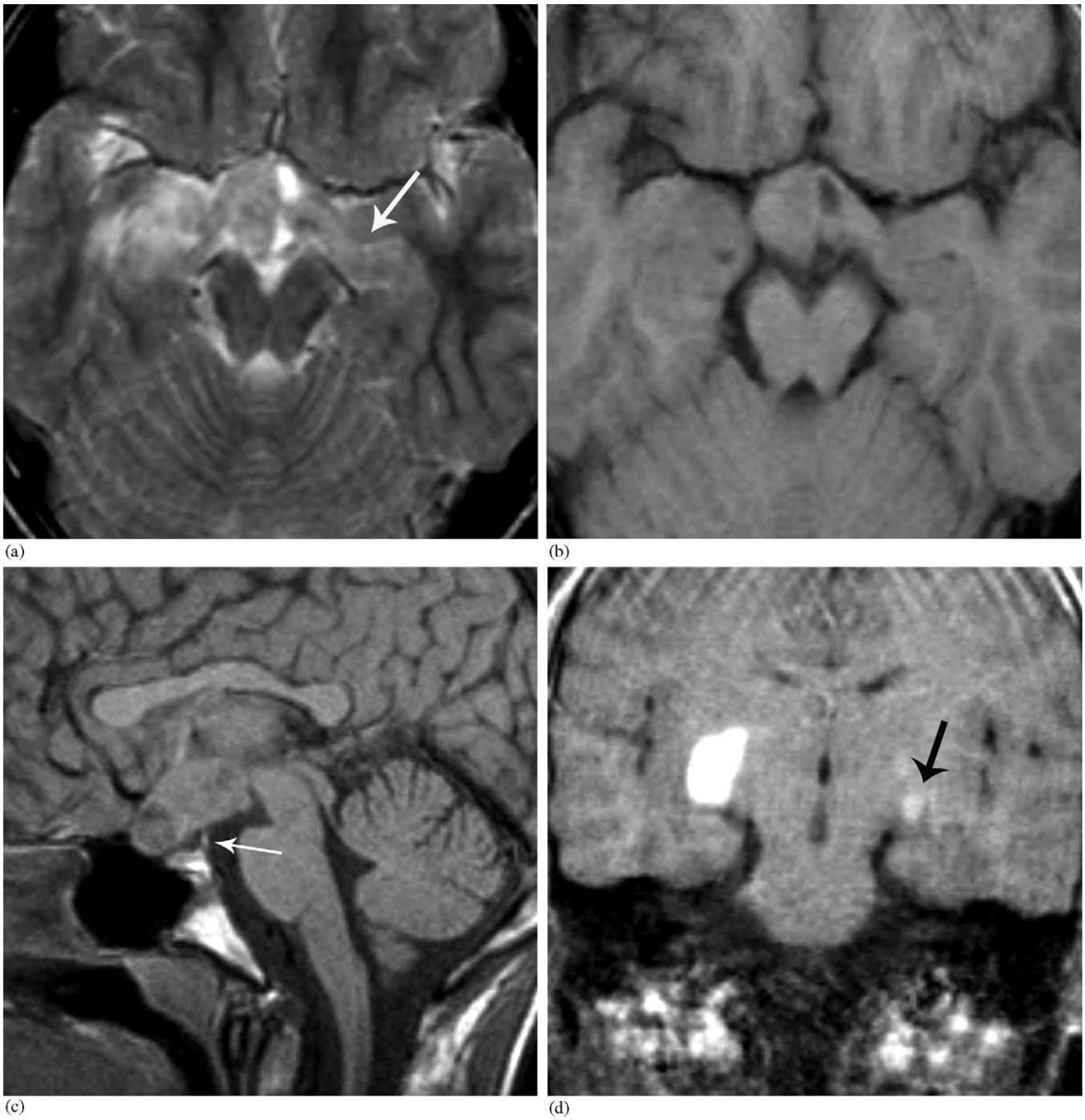

Fig. 16. MR of a 9-year-old boy with pubertas praecox. A bilateral atrophy of the optic nerve and visual deficit were unknown, but found on ophthalmologic examination. Diagnosis: optic glioma with hypothalamic involvement. (a) Axial T2w view, demonstrating hypothalamic and temporomesial infiltration (including the optic tract) of the right side, but another signal enhancement of the left optic tract (arrow). (b) Corresponding T1w native view with enlargement of the right part of the optic chiasm and both optic tracts, with preference to the right. (c) Midsagittal T1w native view, demonstrating a mass without any delineation of the chiasm. The arrow indicates the pituitary stalk. (d) Coronal T1w contrast enhanced view, demonstrating tumor invasion of both lateral geniculate nuclei (arrow), again with preference to the right.

granulomatosis) or secondary in collagen vascular diseases (e.g. systemic lupus erythematosus, rheumatoid arteritis), from infectious (e.g. bacterial, fugal) or non-infectious (e.g. immune-cell-mediated) [12,37]. Clinical symptoms are variable and unspecific, while MR findings may (but not always) show various (although not specific) lesions. As the pathologic process of perivascular inflammation may affect not only capillaries, but also arterioles and arteries simultaneous finding of microinfarctions, territorial and hemodynamic infarctions may occur [36]. Confirmation with cerebral angiography, demonstrating multiple arterial vessel irregularities [12] (Fig. 29), should be aspired.

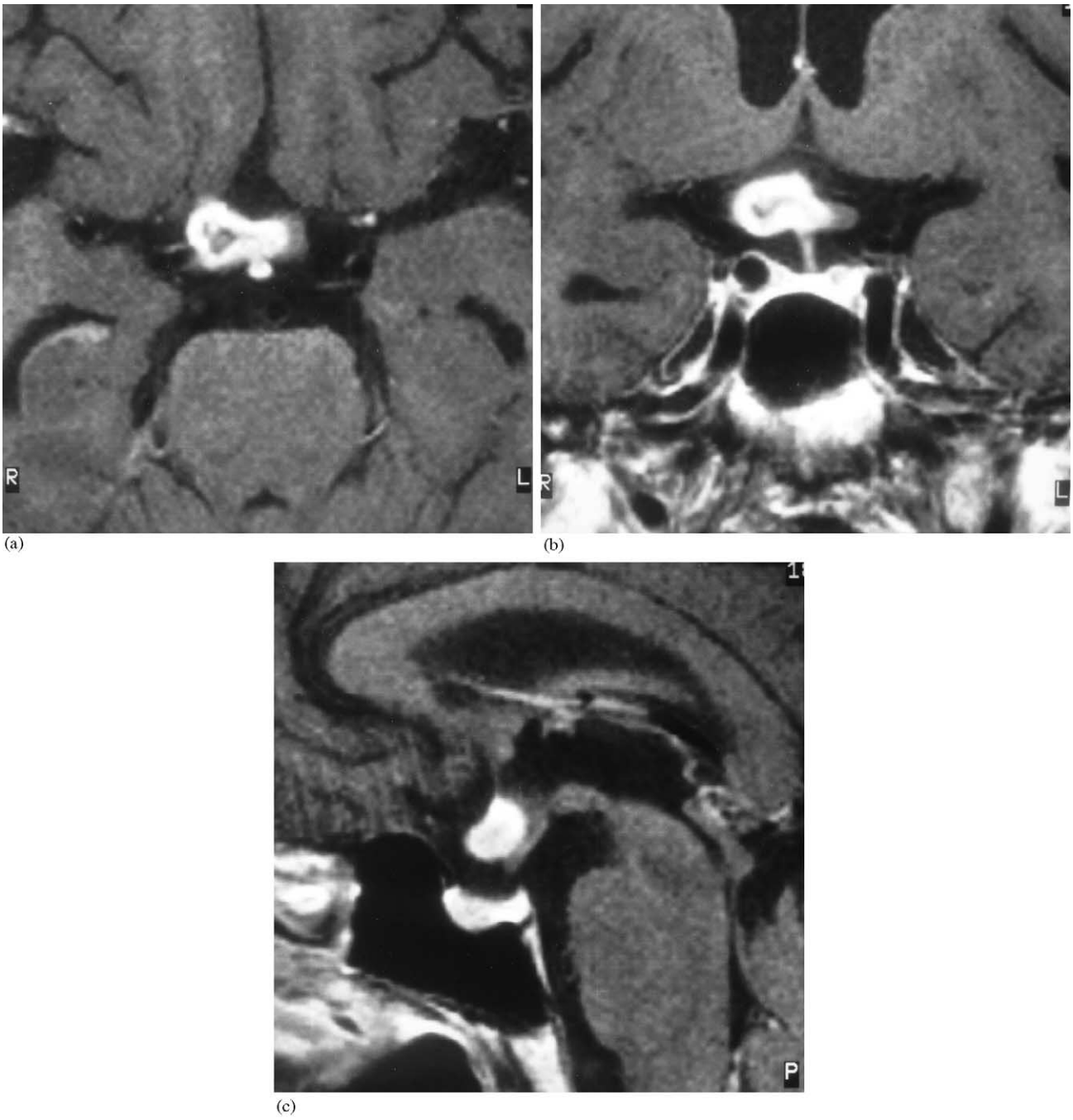

Fig. 17. MR (T1w, contrast enhanced) of a 70-year-old female with progressive visual deficit to loss within 2 weeks of the right eye and loss of vision (o.1) of the left eye. Diagnosis: glioblastoma of the chiasm (a) Axial view with of a solid tumor with some necrosis of the chiasm, demonstrating a lateralization to the right. (b) Coronal view. (c) Midsagittal view, showing beginning invasion of the floor of the third ventricle. (With permission of Müller-Forell, 2002.)

Sturge Weber syndrome (synonym: encephalotrigeminal angiomatosis), a sporadically occurring phacomatosis, is characterized by a 'port wine' stain face (naevus flammeus) in the trigeminal distribution, leptomeningeal venous angiomatosis (caused by faulty development of the venous drainage), clinically presenting with seizures, dementia, hemiplegia, hemianopia, buphthalmus and glaucoma. Intracranial involvement is regularly ispilateral of the nevus flammeus of the face, affecting the occipital lobe preferentially [38]. Although CT can identify (specific) dystrophic subcortical calcification in areas of cortical atrophy, MR is more sensitive than CT in identifying secondary changes of the affected areas, with cortical atrophy, (compensatory) ventricular and choroid plexus enlargement, and calvarial hemiatrophy (Fig. 30). Superficial gyriform contrast enhancement is caused by slowly flowing blood within the

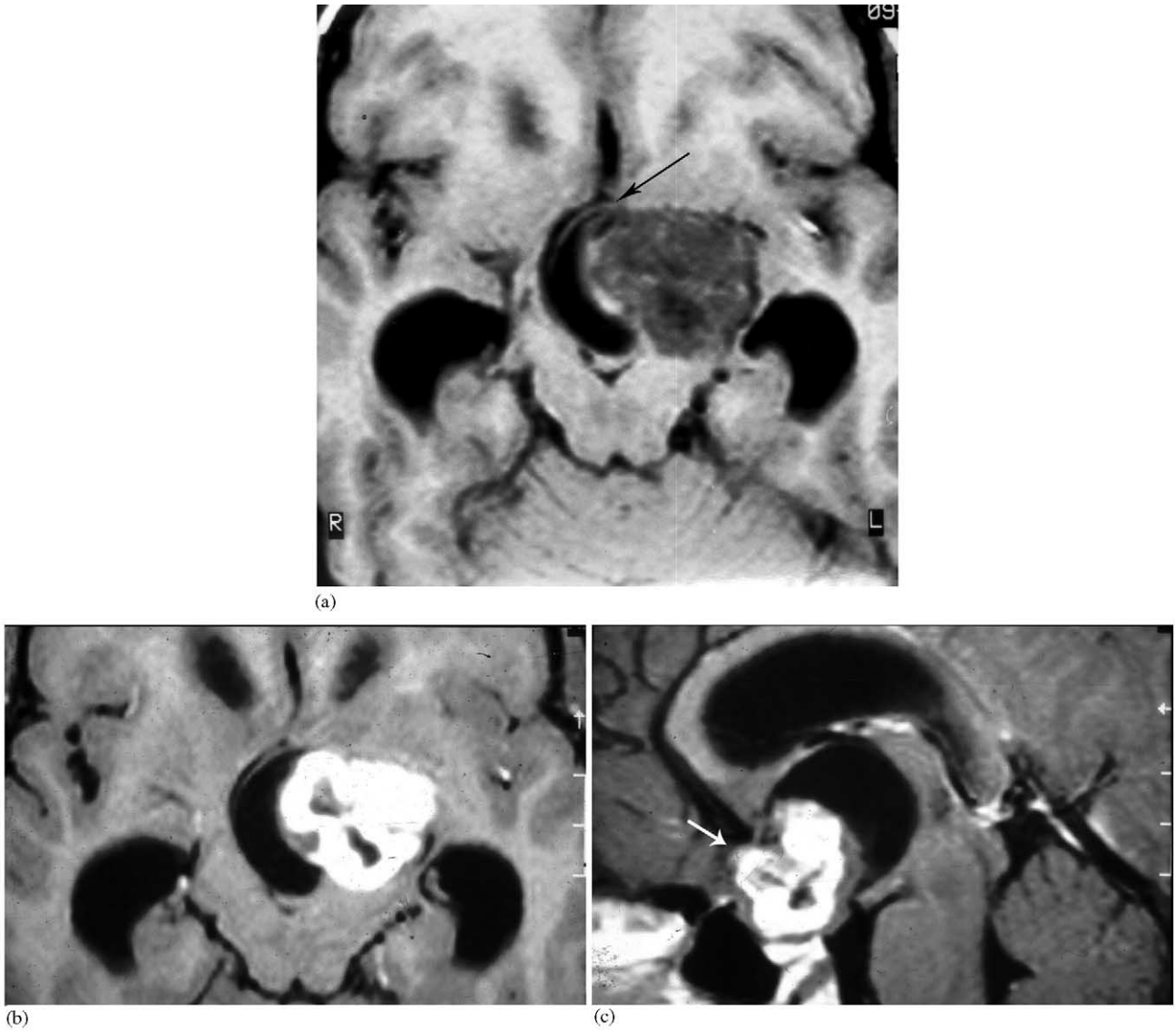

Fig. 18. T1w MR of a 9-year-old boy with known NF1, presented with left N VI paresis and right sided papilledema. Diagnosis: pilocytic astrocytoma of the hypothalamus. (a) Axial view visualising the partly cystic, partly solid tumor in the left hypothalamic region. Note the small capsule, delineating the cystic tumor from the dislocated, impressed third ventricle (arrow). (b) Corresponding contrast enhanced view with bright signal enhancement of the solid tumor part. (c) The midsagittal view shows best the retro-chiasmatic extension of the tumor with caudal impression of the third ventricle. The arrow indicates the chiasm. (With permission of Müller-Forell, 2002.)

persistent plexus of the subarachnoid space and/or BBB loss within cerebral cortex from cerebral ischemia [38].

3.2.2. White matter lesions (MS)

Multiple sclerosis is the most common demyelinating disorder of the CNS. Two main theories concerning the aetiology of this disease are discussed, a genetic and environmental, one might be influenced by the other, so that the expression of a susceptibility gene (or genes) depends on environmental factors [39]. Most often the first and only clinical symptom in younger patients aged from 20 to 40 years, consists of impaired vision, presenting as retro-bulbar neuritis (RBN), followed or combined with fluctuating periods of sensomotoric or gait disturbances [40]. The clinical course of MS can be divided into a relapsing-remitting and a chronic progressive form. MR imaging got a new quality in diagnosis, as new guidelines enable the physician to define the diagnosis for MS, possible MS or nor MS [41]. These guidelines include the evidence of dissemination in time and space of lesions typical for MS, objectively determined by clinical and imaging signs. They should require evidence of at least three of the following findings:

1) one gadolinium enhancing lesion or nine T2-hyperintense lesions,
2) at least one infratentorial lesions
3) at least one juxtacortical lesion
4) at least three periventricular lesions.

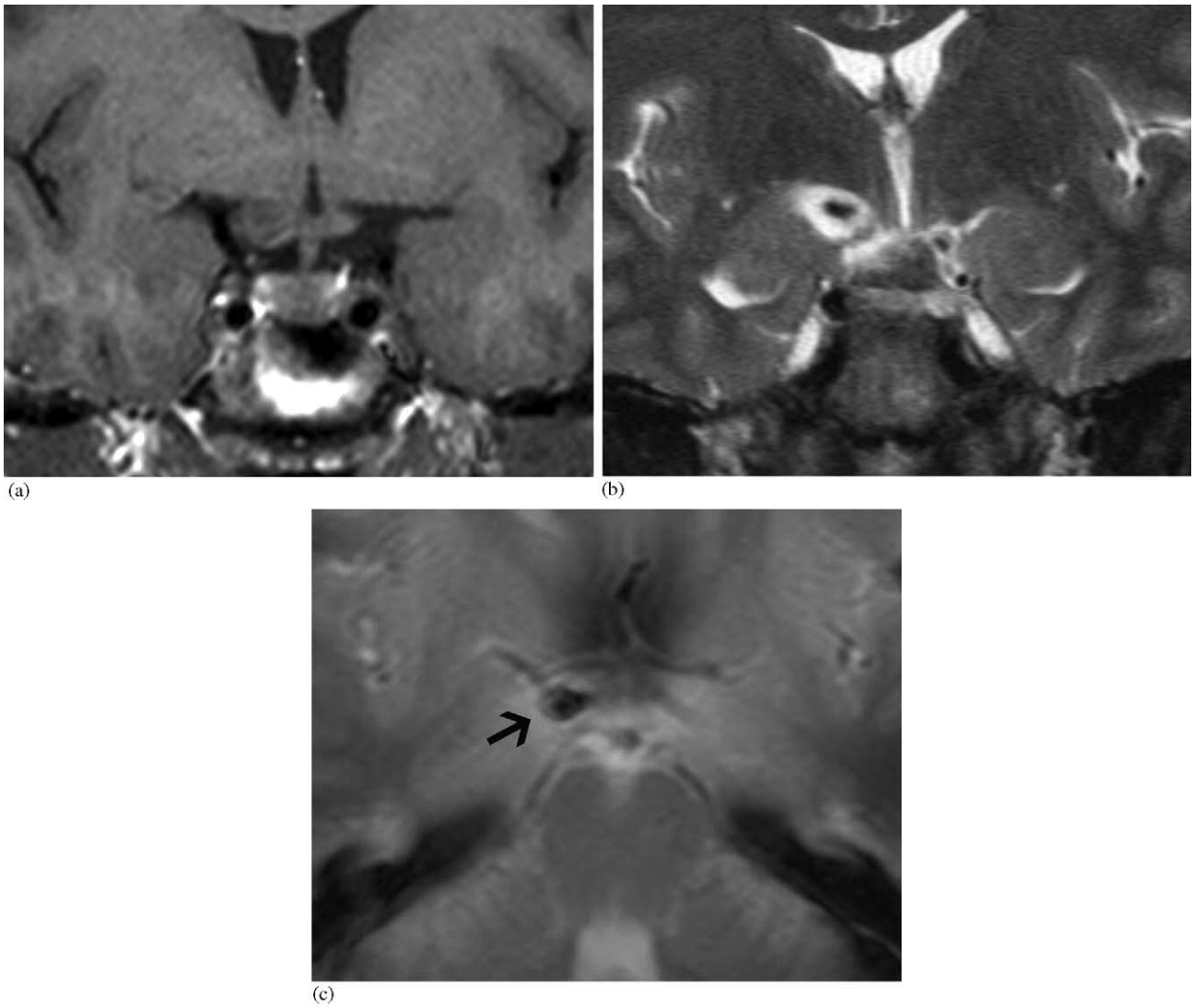

Fig. 19. MR of a 40-year-old female with unspecific symptoms, but no visual deficit. Diagnosis: incidental detected cavernoma of the right chiasm and optic tract. (a) Coronal T1w native view with enlargement of the right chiasm. (b) Coronal T2w image, demonstrating target-like signals at the proximal right optic tract. (c) Axial T2*w image with characteristic hemosiderin susceptibility artefact (arrow).

Additional findings of CSF abnormalities (oligoclonal bands), lymphocytic pleocytosis, and abnormal visual evoked potentials (VEP) provide supplement information to clinical findings, typical for MS.

MR is the imaging tool of choice in suspected demyelinating disorders [8,38–40]. Although the sensitivity in detecting MR lesions is very high, the correlation of neurological symptoms and localization of imaging findings is rare and only probable in some cases (Fig. 31). The imaging protocol should include axial and sagittal PD/T2w and FLAIR sequences, where the demyelinated areas demonstrate a high signal [42]. T1w native and contrast enhanced sequences demonstrate acute or recurrent inflammatory lesions, due to BBB disruption [43]. The sagittal view is best in order to show the characteristic so-called Dawson's finger, presenting as periventricular, pericallosal, ovoid lesions, due to perivascular inflammation in the course of medullary veins [43]. BBB disruption of acute or recurrent inflammatory lesions is apparent in contrast enhanced T1w sequences [43–45].

Acute disseminated encephalomyelitis (ADEM) is characterized by an acute monophasic disorder, in contrary to MS. Predominantly occurring following a viral infection, ADEM may affect patients at any age, but with a preference for children and young adults [46,47]. Consequently, the simultaneous occurrence of a variety of polytopic neurological symptoms such as, e.g. hemi- to tetraplegia or ataxia, combined with optic neuritis and bladder dysfunction may lead to correct diagnosis. The bilateral but slightly asymmetric lesions typically affect both, the white and gray matter, with severe destruction of the latter [39]. The imaging method of choice again is MR, as it best shows the mainly subcortical, confluent foci on T2w images (Fig. 32) and a similar contrast enhancement of all lesions, if BBB disruption is apparent [46,47].

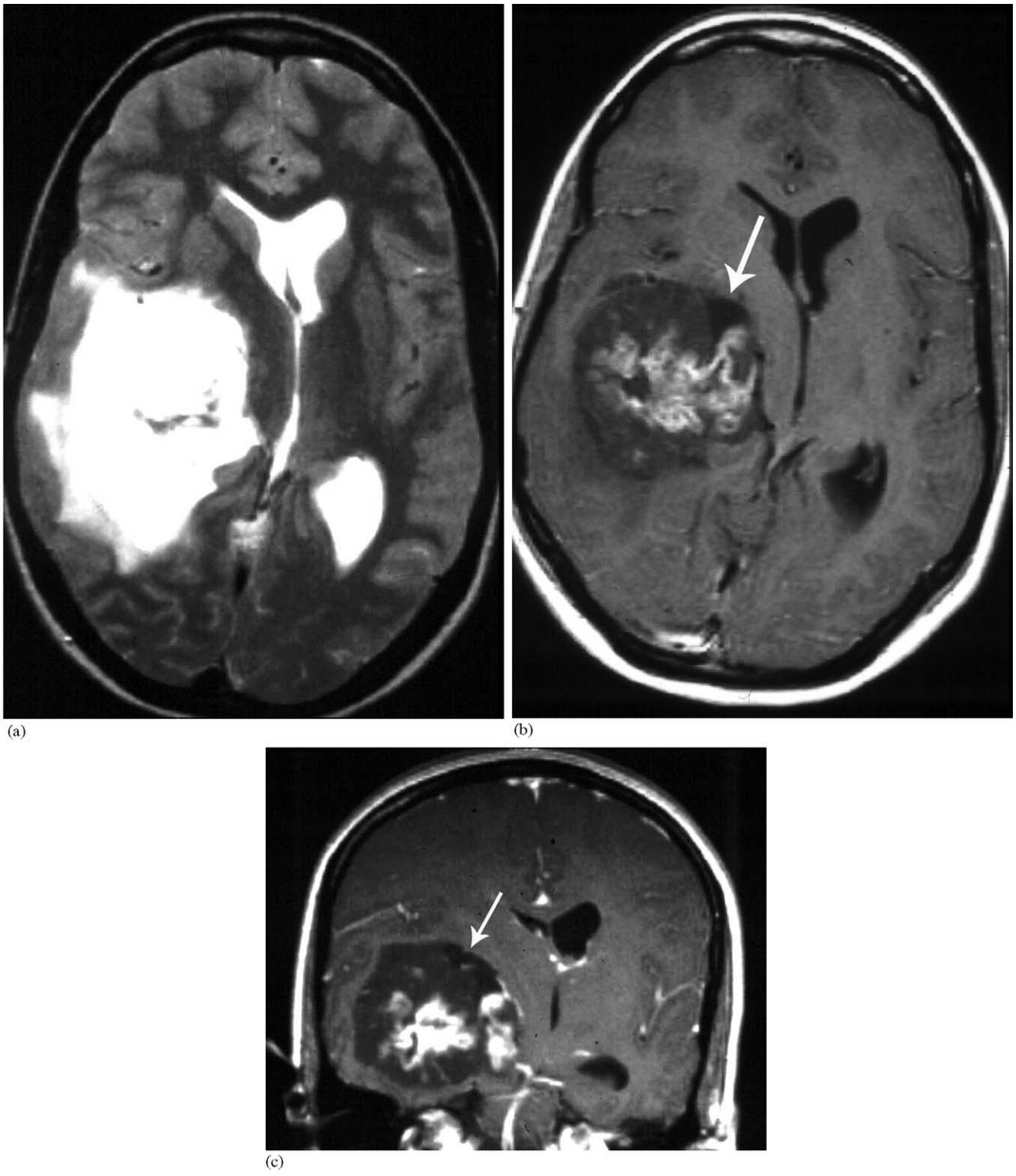

Fig. 20. MR of a 28-year-old woman with chronic headache and slight, unspecific visual disturbances. Diagnosis: intraventricular ependymoma. (a) Axial T2w image with space occupying tumor in the right temporal lobe, only slight perifocal edema. (b) Corresponding T1w contrast enhanced view with inhomogeneous signal enhancement of the tumor. Note the anteriorly displaced temporal horn (arrow) and the distinct delineation of the process, due to mainly intraventricular location. (c) Coronal T1w contrast enhanced view, note the displacement of the temporal horn (arrow). (With permission of Dr Lorenz, Department of Radiology of Katholisches Klinikum Mainz.)

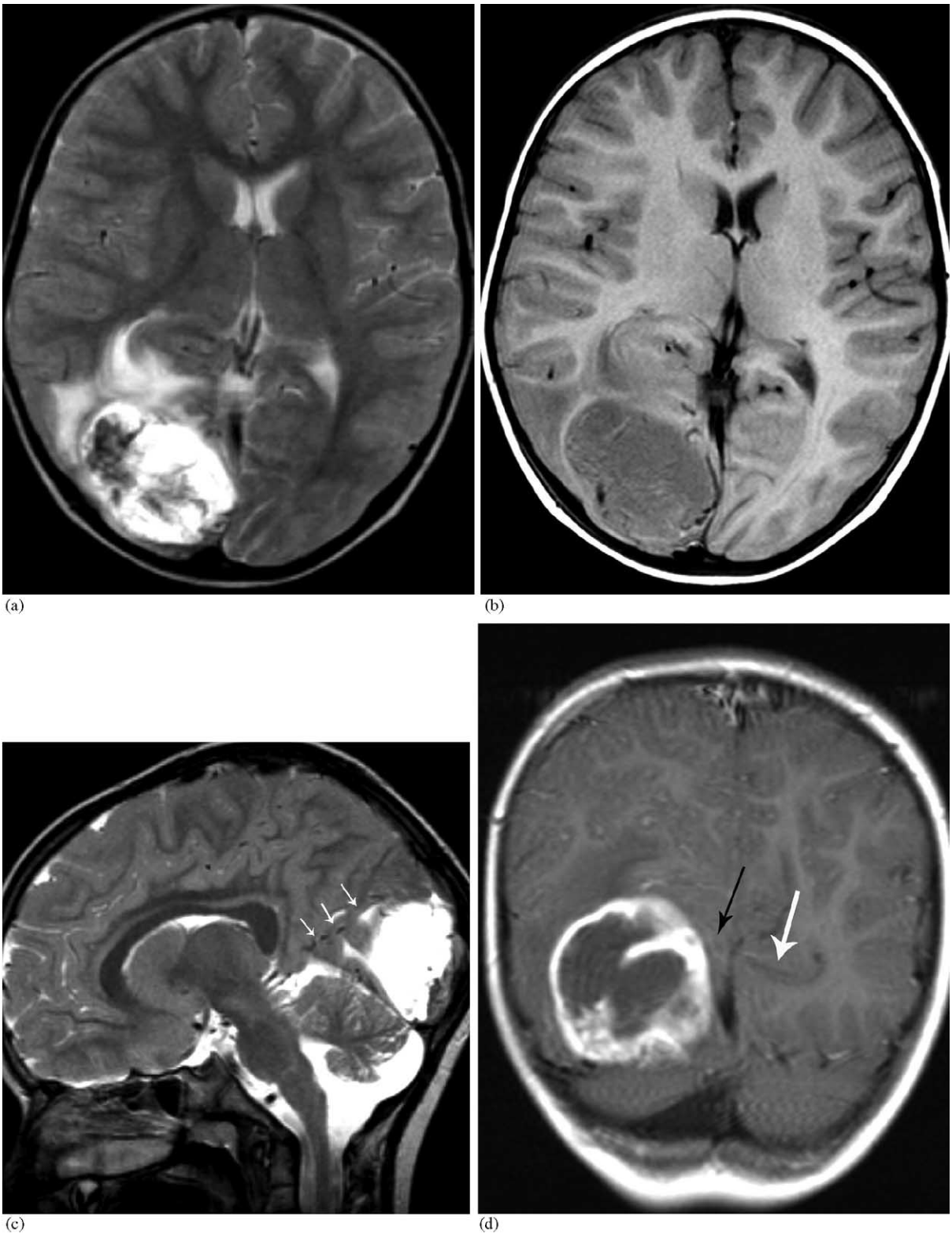

Fig. 21. MR of a 5-year-old boy suffering from headache for 10 days, presenting because of an acute N VI-paresis of the right eye and homonymous hemianopia to the left. Diagnosis: anaplastic ependymoma. (a) Axial T2w view, showing a large mass with apparently cystic configuration (due to tumor necrosis) in the right occipital lobe with compression of the posterior horn of the right ventricle and marked perifocal edema. Note the left optic radiation. (b) Corresponding T1w native view, confirming the suspicion because of the hypointense signal character of the well delineated mass. (c) Paramedian sagittal T2w view. Note the dislocation of the parieto-occipital sulcus (small white arrows) and a widened cerebello-medullary cistern as an incidental finding. (d) Coronal T1w contrast enhanced image, demonstrating the impression of the ispilateral calcarine sulcus (black arrow), compared to the contralateral (white arrow).

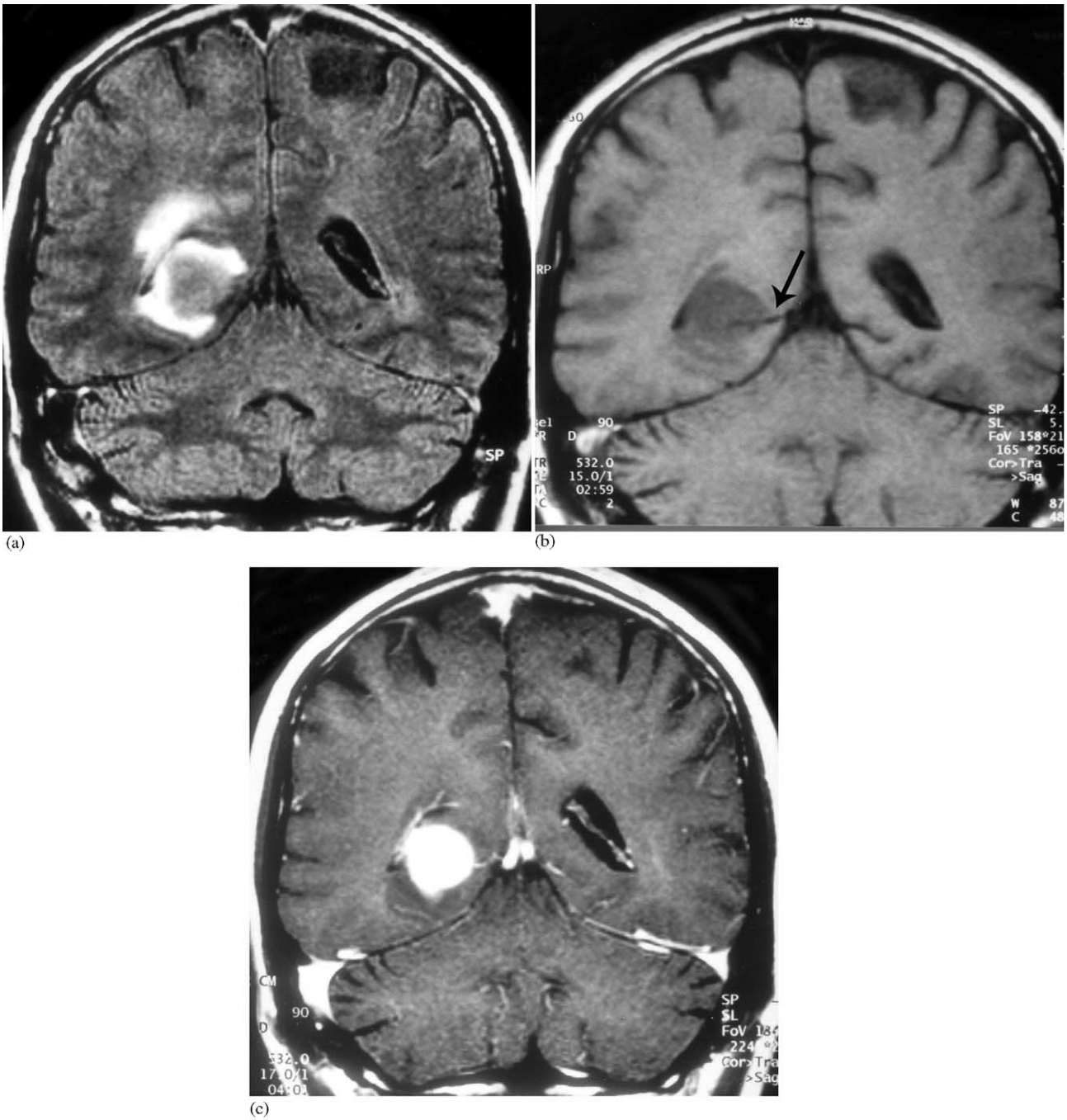

Fig. 22. MR of a 55-year-old man suffering from recurrent blurred vision. Diagnosis: CNS lymphoma. (a) Coronal T2w FLAIR sequence demonstrating the relation of the tumor (intermediate signal) and perifocal edema (bright signal) to the calcarine sulcus. (b) Corresponding T1w native view. The arrow indicates the right calcarine sulcus. (c) Corresponding contrast enhanced view with homogeneous signal enhancement of the lymphoma. (Note the predilection of periventricular location.) ((a) With permission of Müller-Forell, 2002.)

Wernicke encephalopathy is one of multiple exogeneous toxic encephalopathies, caused by a nutritional deficiency of vitamin B (thiamine), mainly, but not exclusively, found in chronic alcoholics. The acute onset of clinical symptoms consists of ophthalmoplegia, ataxia, and confusion, sometimes with additional neuropathy [1,48]. The lesions are distributed symmetrically in the diencephalons along the brainstem, involving the mammillary bodies, the periaqueductal gray matter, and the thalamus, adjacent to the third ventricle (Fig. 33) [1,39]. These pathological findings are reflected on MR, where hyperintensities on T2w images at the periventricular nuclei of the thalami and mamillary bodies are seen, in acute stages combined with contrast enhancement [49].

Sarcoidosis is a systemic granulomatous disease of unknown origin, which present in patients younger than 40 years old, with a slight predilection for women. Patients

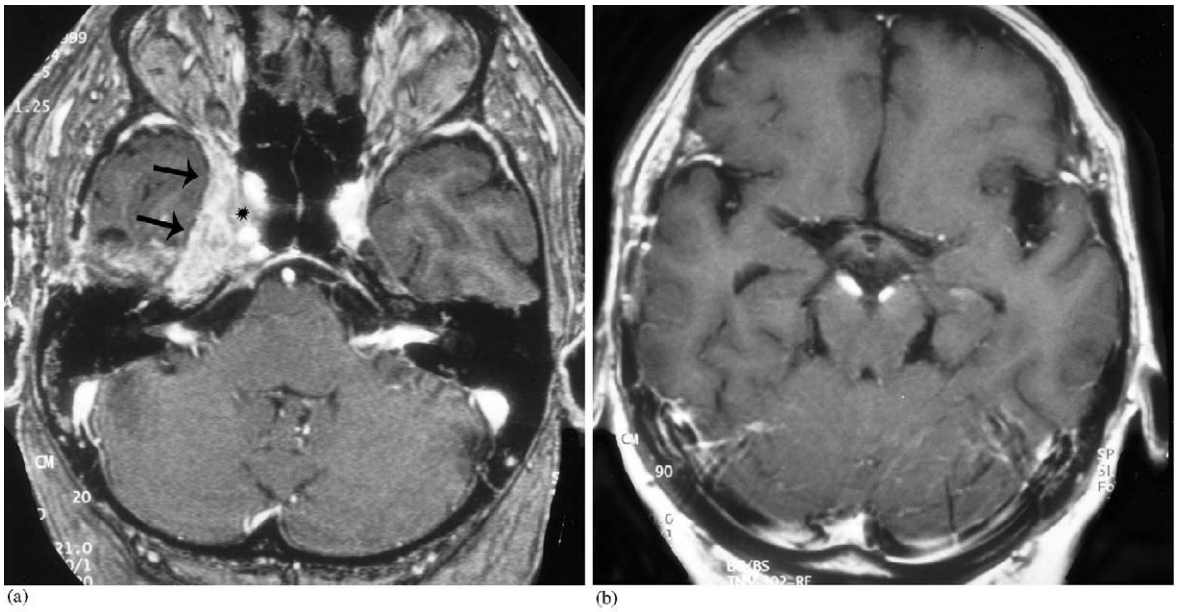

Fig. 23. T1w contrast enhanced MR of a 58-year-old man with acute ptosis of the right eye, deafness, and deficits of several cranial nerves. Diagnosis: primary CNS lymphoma. (a) Axial view at the level of the internal auditory canal, demonstrating tumor involvement of both N VII/N VIII nerve complexes and a wide meningeal tumor of the right middle cranial fossa with infiltration of the cavernous sinus (arrows). (b) Axial view at the level of the chiasm shows significant signal enhancement of the leptomeningeal tumor-coating of both oculomotor nerves in the interpeduncular cistern. (With permission of Müller-Forell, 2002.)

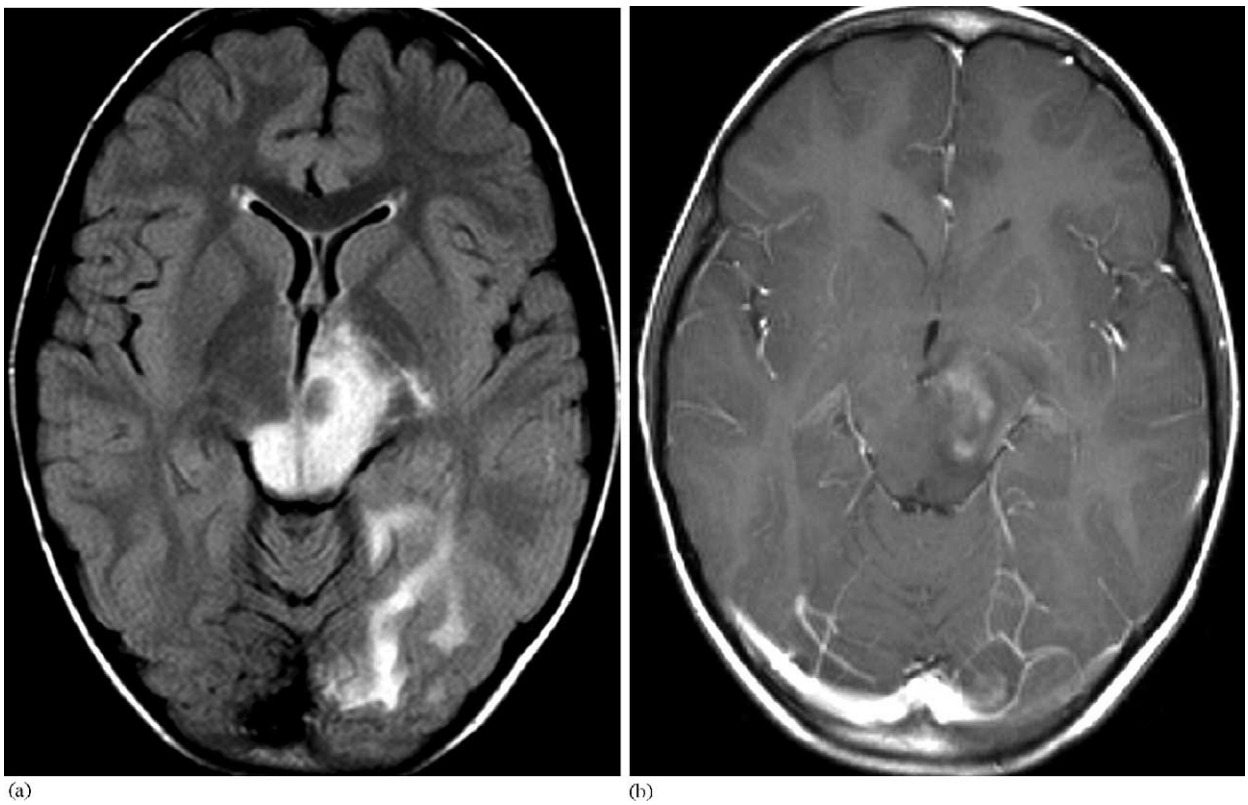

Fig. 24. MR of a 9-year-old boy with known ALL, presenting with acute N VI-paresis and progressive loss of consciousness. Diagnosis: extensive intracranial metastasis of extracranial ALL. (a) Axial FLAIR image with mesencephalic and left thalamic infiltration and additional subcortical edema of the left calcarine region. (b) Corresponding T1w contrast enhanced view with only little signs of BBB-disruption. (c) The coronal T1w contrast enhanced view some minutes later demonstrates an intense enhancement in the left occipital lesion, and an additional in the ipsilateral parietal lobe.

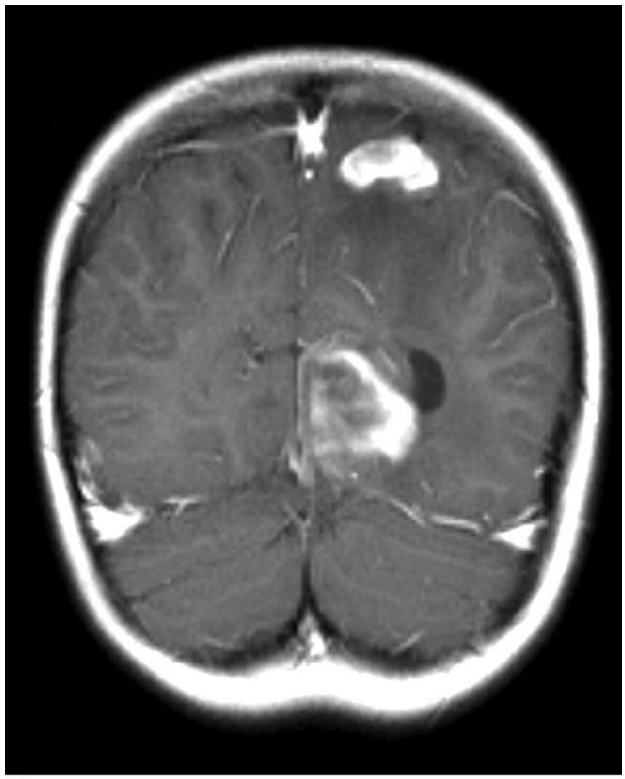

(c)

Fig. 24. (*Continued*).

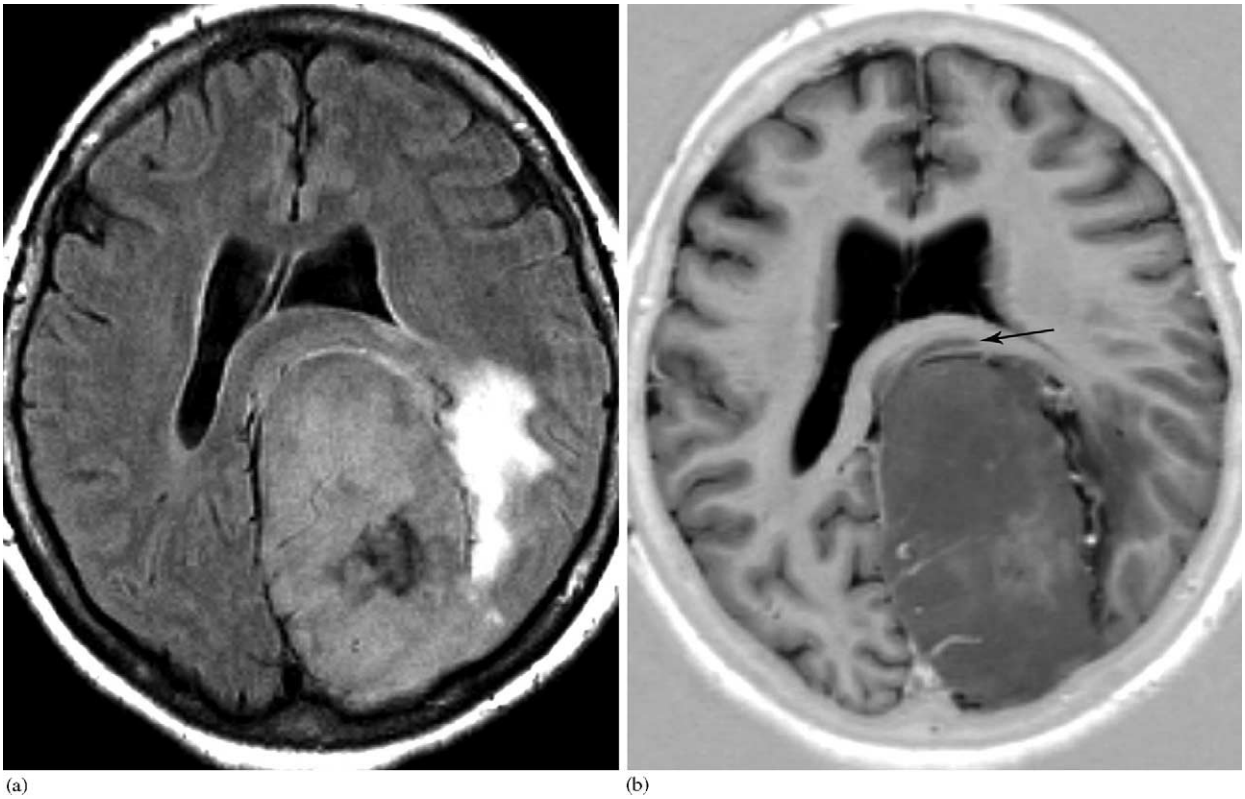

(a) (b)

Fig. 25. MR of a 65-year-old female presenting with seizure and homonymous hemianopia to the right. Diagnosis: left occipital meningeoma. (a) Axial flair image with large mass in the left occipital region. Note the slightly inhomogeneous signal with central hypointensity (corresponding calcification) and some perifocal edema. (b) Corresponding T1w (IR) view, where the extrinsic character of the tumor is apparent, with compression of the parahippocampal gyrus (arrow) and splenium of the corpus callosum. (c) Corresponding contrast enhanced image. Note the hypointensity of the calcified portion. (d) Coronal T1w (IR) view; the calcarine sulcus and visual cortex (arrow) is extremely dislocated.

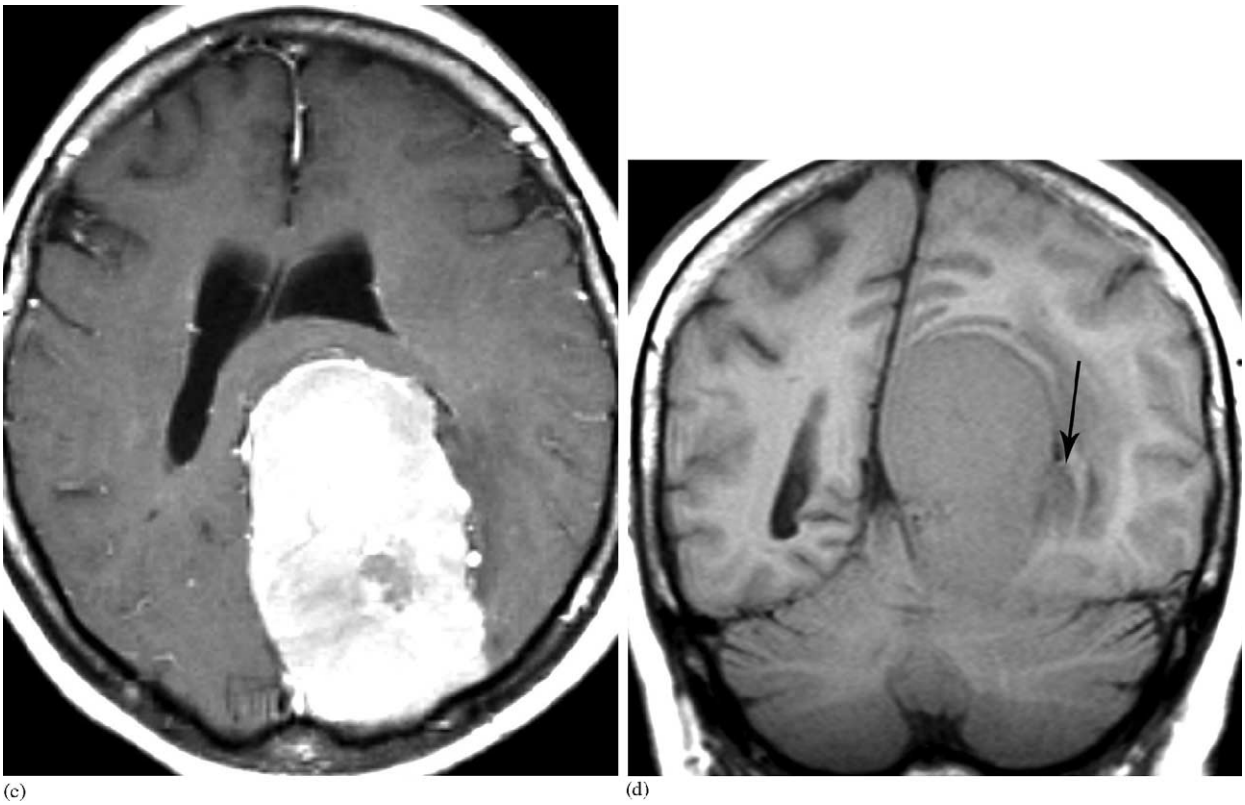

(c) (d)

Fig. 25. (*Continued*).

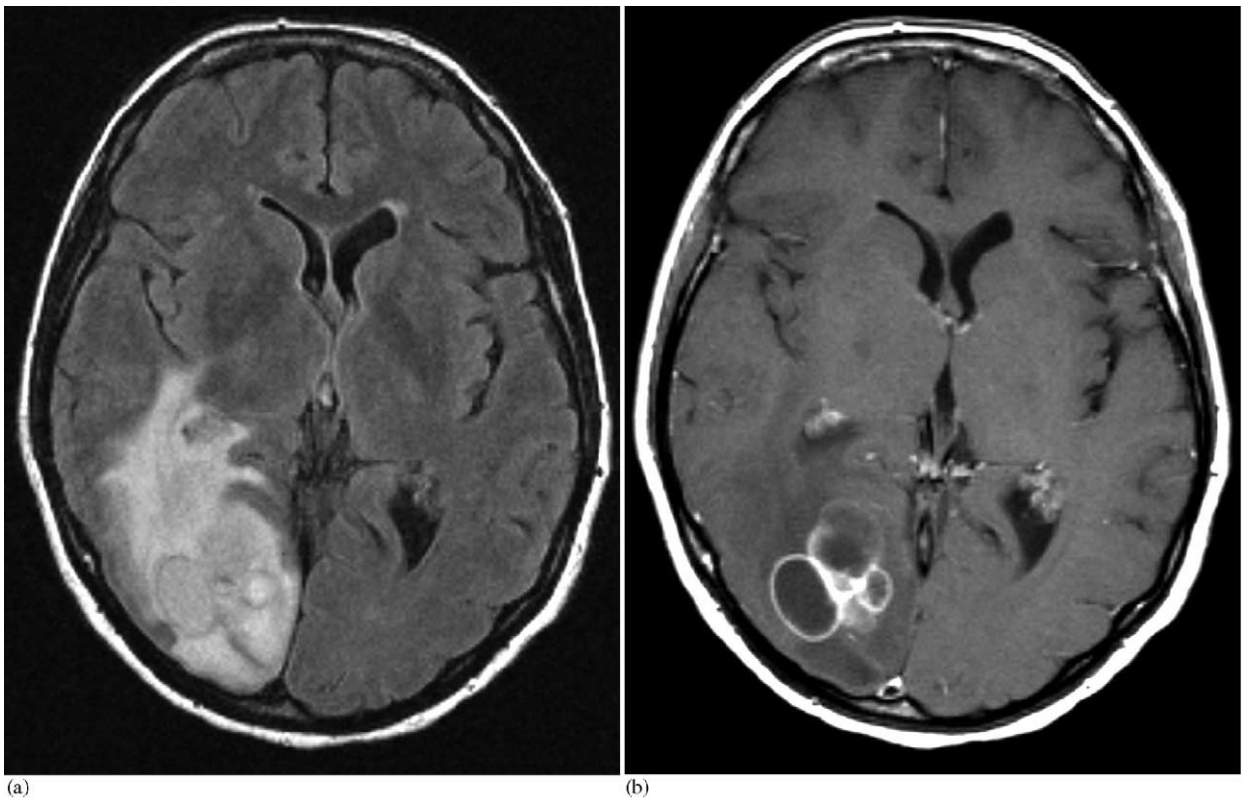

(a) (b)

Fig. 26. MR of a 48-year-old female presenting chronic headache since two months and with homonymous hemianopia to the left. Diagnosis: metastasis of a (up to date) unknown carcinoma of the kidney. (a) Axial FLAIR image with a mixed (solid and cystic) structure in the posterior part of the occipital lobe and extensive edema. (b) Corresponding T1w contrast enhanced view, with enhancement of the solid parts of the tumor.

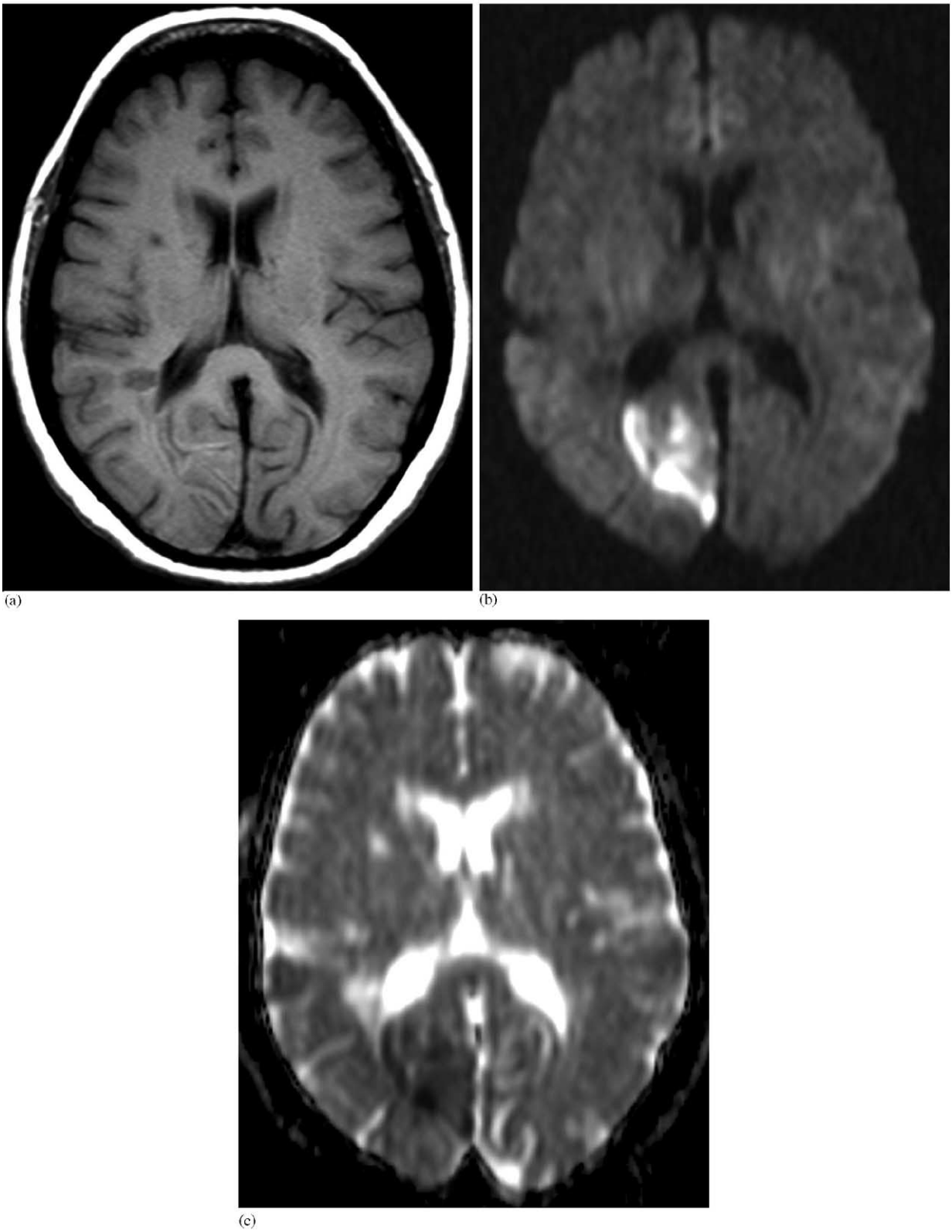

Fig. 27. MR of a 57-year-old woman presenting with acute homonymous hemianopia to the left. Diagnosis: acute infarction of the right PCA (posterior cerebral artery). (a) Axial T1w native view with diffuse swelling of the right occipital gyri adjacent to calacarine sulcus, and with additional subcortical hemorrhagic transformation. (b) Corresponding DWI with bright signal. (c) Corresponding ADC map, demonstrating the acute infarction by hypointensity of the affected area.

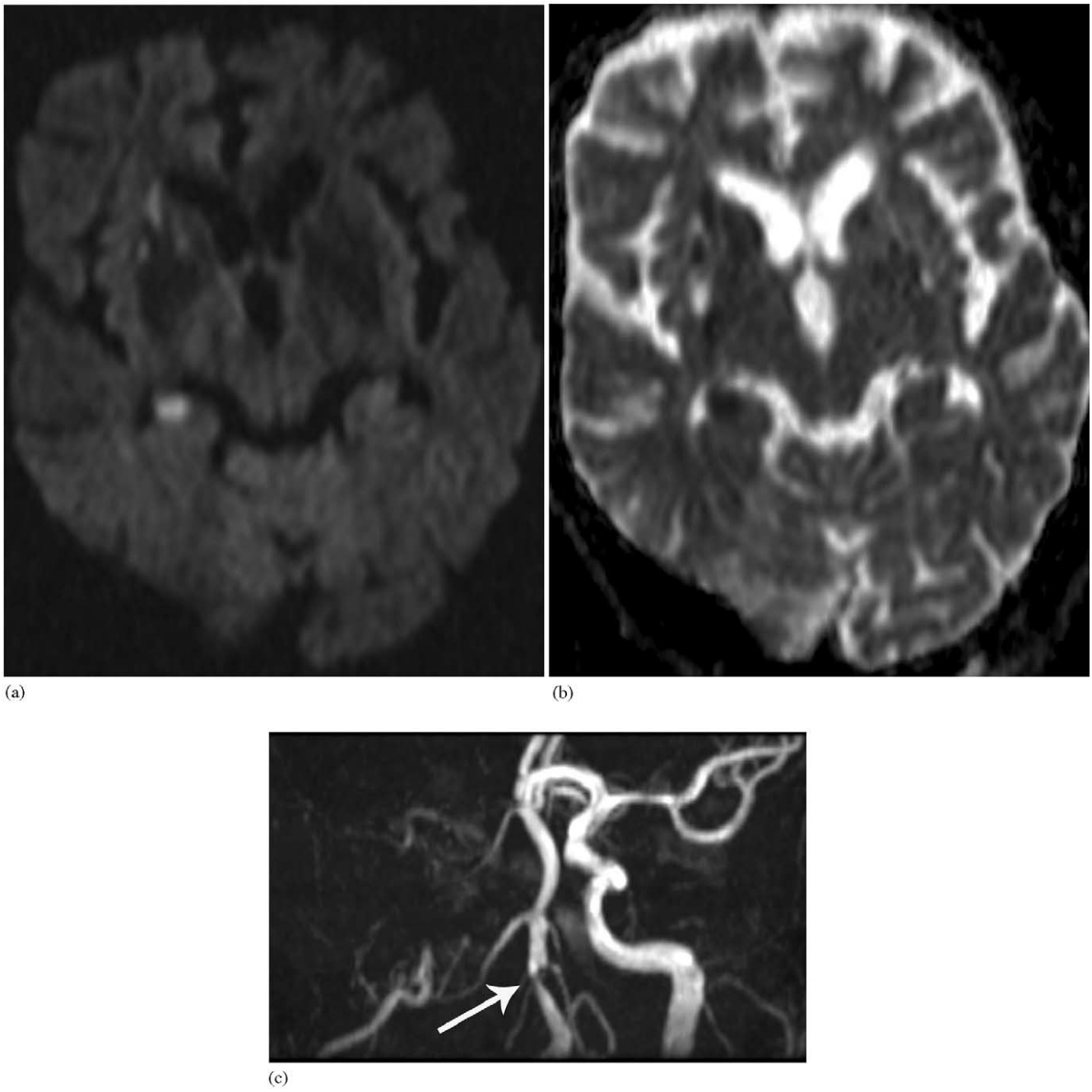

Fig. 28. MR of a 70-year-old man, with known occlusion of the right ICA, who presents with acute homonymous hemianopia to the left. Diagnosis: embolic infarction of the right geniculate nucleus. (a) DWI, showing another (subacute) infarction of the anterior basal ganglia. (b) Corresponding ADC map. (c) 3D-MRA (TOF), where the total occlusion of the right ICA is apparent and additional stenosis of the left vertebral artery (V4-segment) (arrow) is apparent.

present with anergy, clinical symptoms include a positive Kveim test, hilar adenopathy, hypercalcemia and uveitis. In up to 10%, an involvement of the CNS is evident, in rare cases as the first or only clinical manifestation [50]. Histopathology consist of noncaseating granulomas, mostly around the basal cisterns, with preference to the cranial nerves, including optic chiasm as the most common site of affection [1], in rare cases with an intraparenchymatous extension via the Virchow-Robin-spaces (Fig. 34).

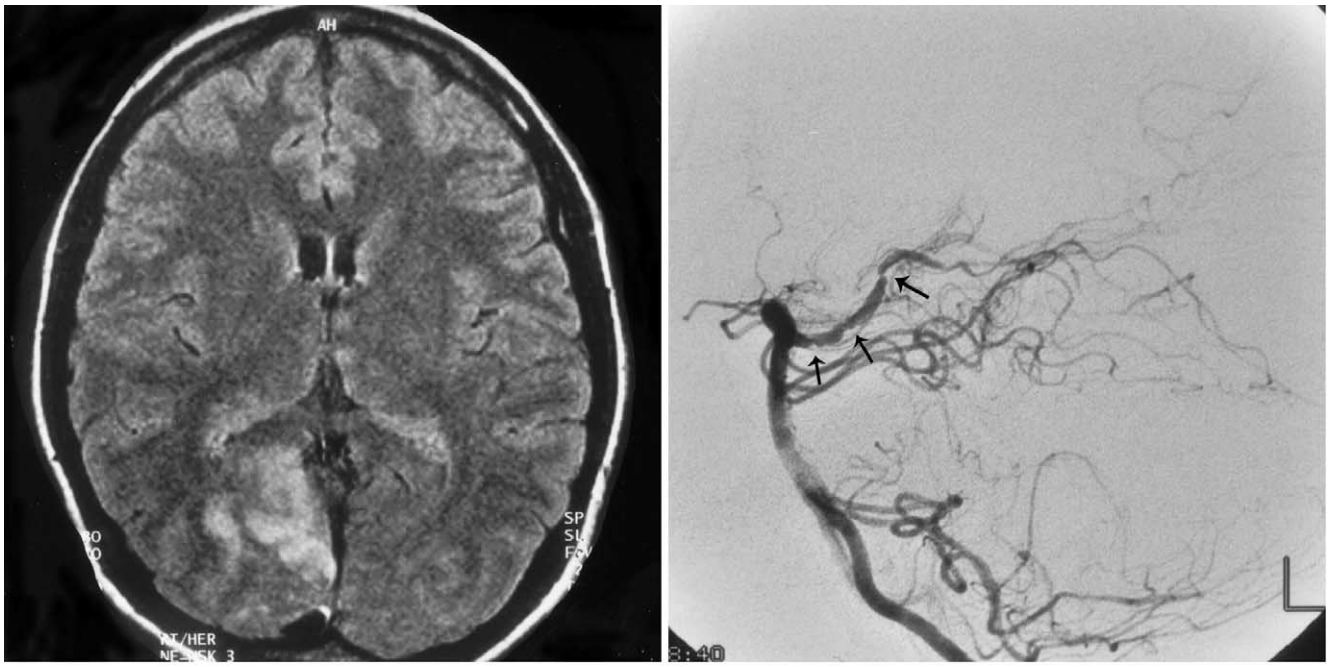

(a) (b)

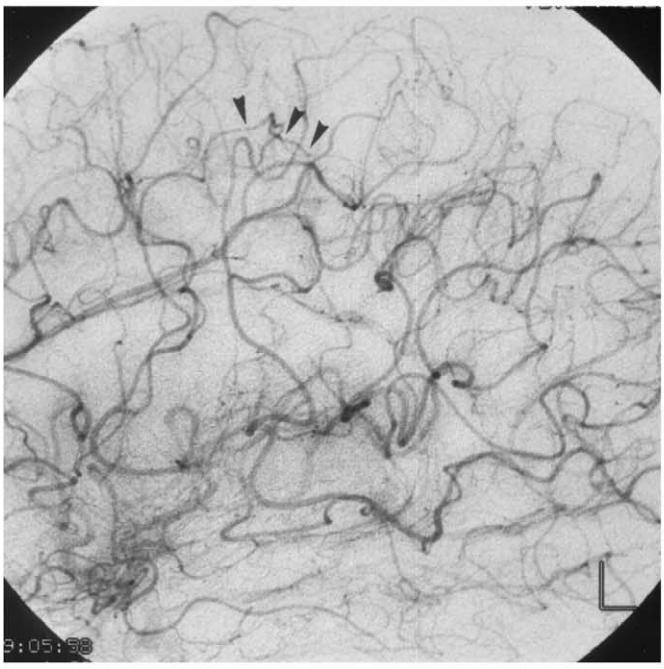

(c)

Fig. 29. A 33-year-old woman with acute homonymous hemianopia to the left. Diagnosis: infarction of PCA associated with cerebral vasculitis. (a) MR: axial T2w FLAIR image with an area of high signal intensity in the calcarine region. (b) Intra-arterial DSA: early lateral-view of the left VA (vertebral artery) with clearly apparent irregularity with narrowing (arrowhead) and fusiform widening of the PCA in the entire distribution area. (c) Arterial phase of the left ICA in lateral view, confirming the diagnosis by segmental irregularity (arrowheads) of the distal branches of the MCA (middle cerebral artery). (With permission of Müller-Forell, 2002.)

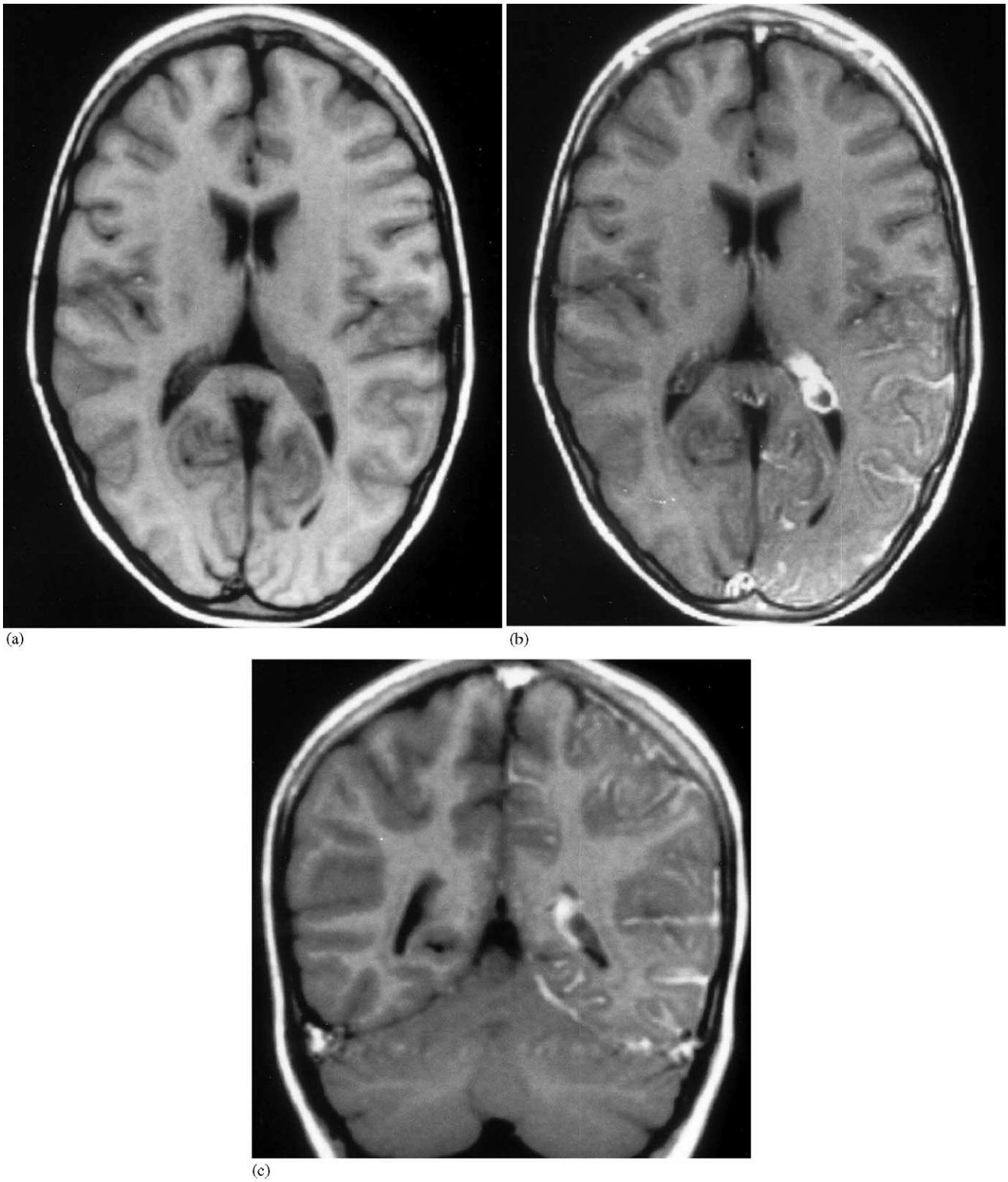

Fig. 30. MR of an 11-year-old girl with unexplained unconsciousness and known Sturge-Weber syndrome. (a) Axial T1w native view without any evident abnormality. (b) Corresponding contrast enhanced view, demonstrating leptomeningeal enhancement of the left temporo-occipital region as well as thickening of and asymmetric enhancement of the ispilateral choroid plexus. (c) Coronal T1w contrast enhanced view. Note the slight thickening and enhancement at the tentorium. (With permission of Müller-Forell, 2002.)

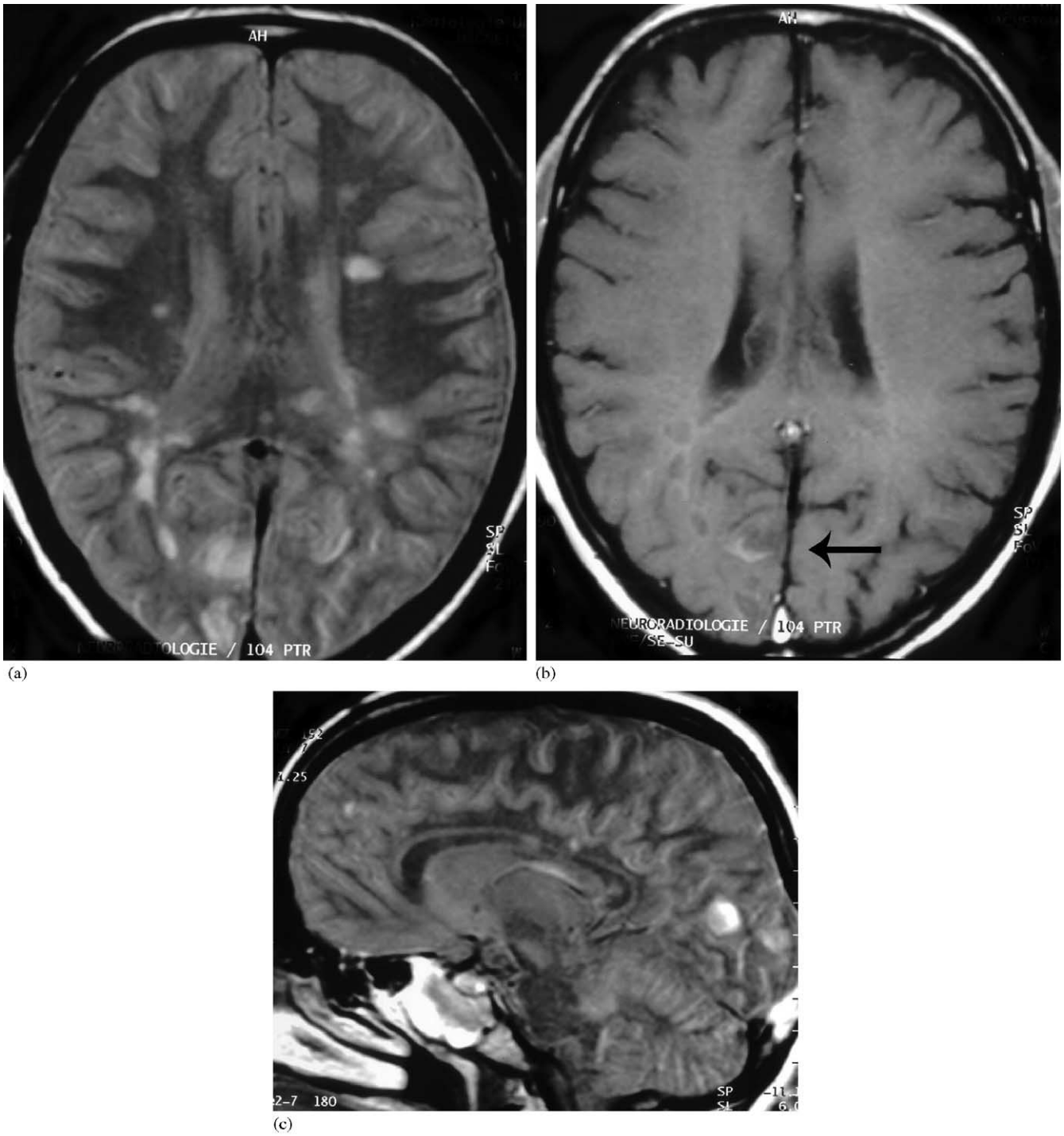

Fig. 31. MR of a 30-year-old female with recurrent optic neuritis and alternating neurological deficits. Diagnosis: multiple sclerosis. (a) Axial PDw image, demonstrating multiple, typical ovoid periventricular lesions with preference to the occipital region. (b) Corresponding T1w contrast enhanced view, where a slight BBB disruption is seen adjacent to the right calcarine sulcus (arrow). (c) Paramedian sagittal PDW image, showing a demyelinating plaque not only in the striate area but in the frontal white matter and in the corpus callosum.

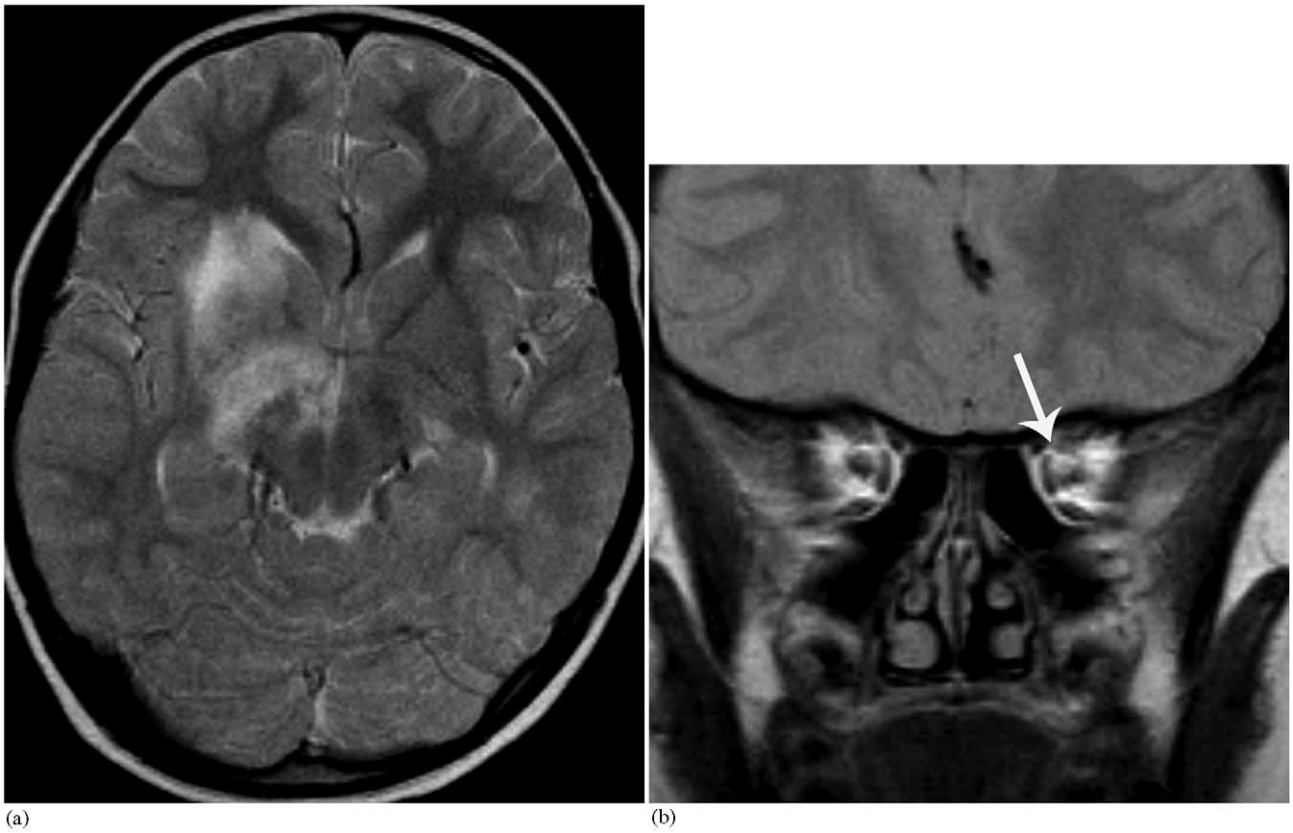

(a) (b)

Fig. 32. MR of a 6-year-old boy with acute (not longer than 12 h) bilateral vision loss, and acute, diffuse disseminating pain in all parts of the body. Diagnosis: ADEM (acute disseminating encephalomyelitis). (a) Axial T2w view, demonstrating inflammatory affection of both optic tracts towards the lateral geniculate nucleus (right»left), right thalamus and basal ganglia. (b) Coronal T2w view of the posterior orbit with bright signal enhancement of the left optic nerve.

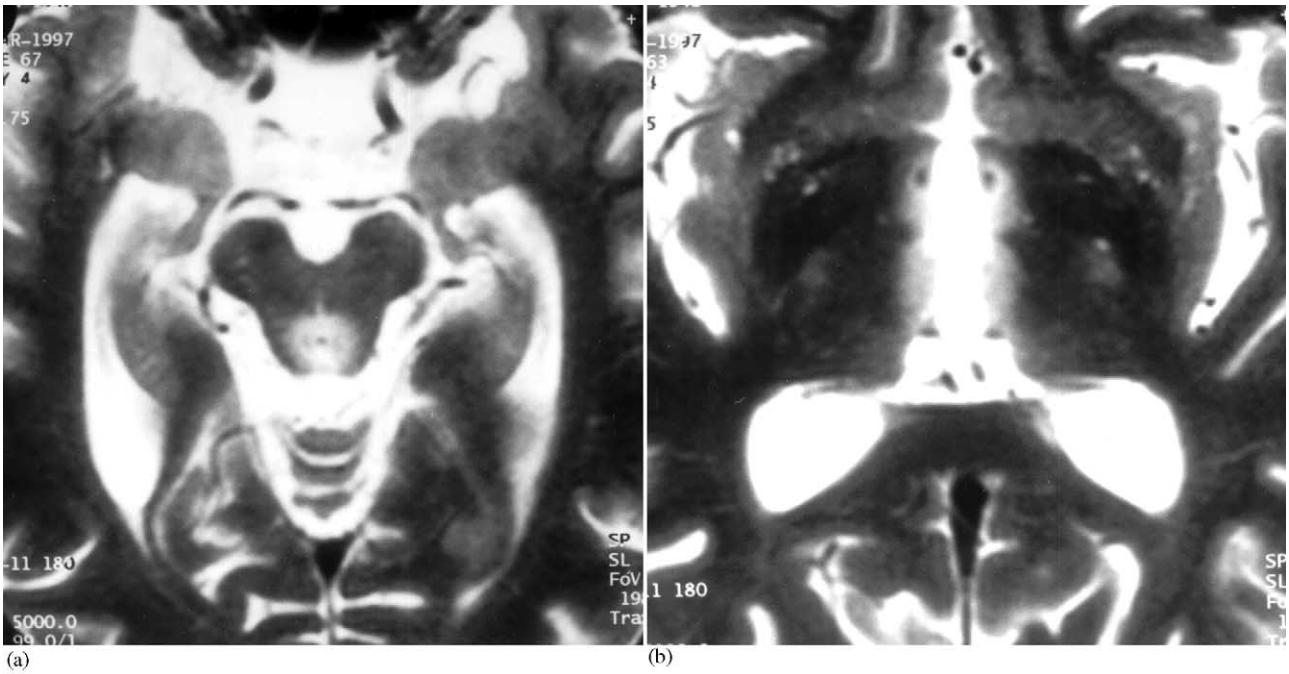

(a) (b)

Fig. 33. T2w MR of a 47-year-old woman alcoholic presenting with bilateral internuclear ophthalmoplegia (INO) and ataxia. Diagnosis: Wernicke encephalopathy. (a) Axial view of the cerebral peduncle showing the characteristic periaqueductal demyelination. (b) Axial view of the region of the third ventricle demonstrates the periventricular involvement (thalami). (With permission of Müller-Forell, 2002.)

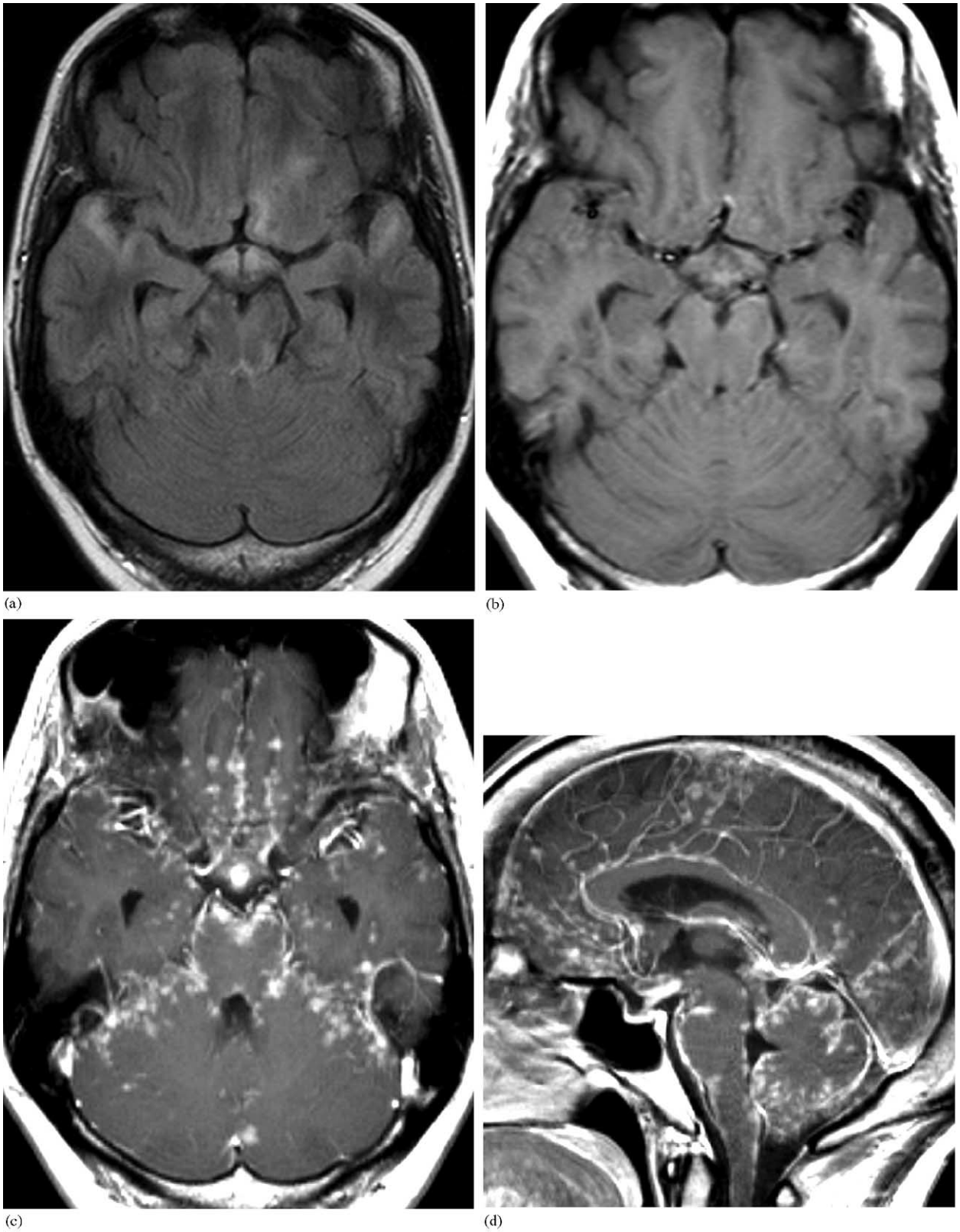

Fig. 34. MR of a 31-year-old female presenting with seizure, hypakusis, ptosis and internuclear ophthalmoplegia (INO) of the right eye. Diagnosis: sarcoidosis: (a) Axial T2w FLIR image with high signal of the chiasm and adjacent frontal as well as bitemporal subcortical white matter. (b) Corresponding T1w native view with irregular signals in the basal cistern. (c) Corresponding contrast enhanced view demonstrating ubiquitous nodular and confluent signal enhancement in all basal cisterns with interpeduncular dominance. (d) Midsagittal T1w contrast enhanced view, showing that the entire subarachnoid space is affected.

References

[1] Okazaki H. Fundamentals of neuropathology. Morphologic basics of neurologic disorders. New York: Igaku-Shoin, 1989.

[2] Goldberg HI, Lavi E, Atlas SW. Tumors. In: Atlas SW, editor. Magnetic resonance imaging of the brain and spine. 2nd ed. Philadelphia: Lippincott-Raven; 1996, p. 423–87.

[3] Müller-Forell W. Imaging of orbital and visual pathway pathology. Springer, 2002.

[4] Osborn A, Rauschning W. Brain tumors and tumorlike masses: classification and differential diagnosis. In: Osborn A, editor. Diagnostic neuroradiology. St. Louis: Mosby; 1994, p. 401–528.

[5] Kucharczyk W, Montanera W, Becker LE. The sella turcica and parasellar region. In: Atlas SW, editor. Magnetic resonance imaging of the brain and spine. Philadelphia: Lippincott-Raven; 1996, p. 871–930.

[6] Dietemann JL, Kehrli P, Maillot C, Dinz R, Reis M, Neugroschl C, Vinclair L. Is there a dural wall between the cavernous sinus and the pituitary fossa? Anatomical and MRI findings. Neuroradiology 1998;40:627–30.

[7] Louis DN, Scheithauer BW, Budka H, van Deimling A, Kepes JJ.Meningiomas. In: Kleihues P, Cavanee WK, editors. Pathology and genetics. Tumors of the nervous system. International Agency for Research on Cancer, Lyon; 2000, p. 176–84.

[8] Sartor K. MR imaging of the skull and brain. A correlative atlas. Springer, 1992.

[9] Crotty TB, Scheithauer BW, Young Jr, WF, David DH, Shaw EG, Miller GM, Burger PC. Papillary craniopharyngeoma: a clinical study of 48 cases. J Neurosurg 1995;83:206–14.

[10] Kleihues P, Burger PC, Scheithauer BW.. Histological typing of tumors of the central nervous system. In: World Health Organization International Histological Classification of Tumors. 2nd ed. Springer, 1993.

[11] Sartoretti-Schefer S, Wichmann W, Aguzzi A, Valavanis A. MR differentiation of adamantinous and squamous-capillary cranipopharyngeoma. AJNR Am J Neuroradiol 1997;18:77–87.

[12] Osborn A.Stroke. In: Osborn A, editor. Diagnostic neuroradiology. St. Louis: Mosby; 1994a, p. 330–98.

[13] Stehbens WE. Cerebrovascular disease. In: Stehbens WE, Lie JT, editors. Pathology of the cerebral blood vessels. Vascular pathology. London: Chapman & Hall; 1995, p. 437–88.

[14] Kupersmith MJ.Aneurysms involving the motor and sensory visual pathway. In: Kupersmith MJ, editor. Neurovascular neuroophthalmology. Springer; 1993, p. 239–99.

[15] Wilcock D, Jaspan T, Holland I, Cherryman G, Worthington B. Comparison of magnetic resonance angiography with conventional angiography in the detection of intracranial aneurysms in patients presenting with subarachnoid hemorrhage. Clin Radiol 1996;51:330–4.

[16] Byrne JV, Guglielmi G. Endovascular treatment of intracranial aneurysms. Springer, 1998.

[17] Sugahara T, Korogi Y, Nagashima K, Hamatake S, Honda S, Takahashi M. Comparison of 2D and 3D digital subtraction angiography in evaluation of intracranial aneurysms. AJNR Am J Neuroradiol 2002;23:1545–52.

[18] Rosenblum MK, Matsutani M, Van Meir EG. CNS germ cell tumors. In: Kleihues P, Cavanee WK, editors. Pathology and genetics. Tumors of the nervous system. Lyon: International Agency for Research on Cancer; 2000, p. 208–14.

[19] Meyers SP, Hirsch WL, Curtin HD, Barnes L, Sekhar LN, Sen C. Chordomas of the skull base: MR features. AJNR Am J Neuroradiol 1992;13:1627–36.

[20] Dutton JJ. Gliomas of the anterior visual pathway. Surv Ophthalmol 1994;38:427–52.

[21] Wulc AE, Bergin DJ, Barnes D, Scaravilli F, Wright JE, McDonald WI. Orbital optic nerve glioma in adult life. Arch Ophthalmol 1989;107:1013–6.

[22] Hollander MD, FitzPatrick M, O′Connor SG, Flanders AE, Tartaglino LM. Optic gliomas. Radiol Clin North Am 1999;37:59–71.

[23] Cavanee WK, Furnari FB, Nagane M, Huang HJS, Newcomb EW, Bigner DD, Weller M, Berens ME, Plate KH, Israel MA, Noble MD, Kleihues P.Diffusely infiltrating astrocytomas. In: Kleihues P, Cavanee WK, editors. Pathology and genetics of tumors of the central nervous system. Lyon: IARC Press; 2000, p. 10–21.

[24] Kleihues P, Burger PC, Collins VP, Newcomb EW, Ohgaki H, Cavanee WK. Glioblastoma. In: Kleihues P, Cavanee WK, editors. Pathology and genetics. Tumors of the nervous system. Lyon: International Agency for Research on Cancer; 2000, p. 29–39.

[25] Aoki S, Barkovich AJ, Nishimura K, Kjos BO, Macida T, Cogen P, Norman D. Neurofibromatosis types 1 and 2: cranial MR findings. Radiology 1989;172:527–34.

[26] Steiger HJ, Markwalder TM, Reulen HJ. Clinicopathological relations of cerebral cavernous angiomas. Observation in eleven cases. Neurosurgery 1987;21:879–84.

[27] Kupersmith MJ, Kalish H, Epstein F, Yu G, Berenstein A, Woo H, Jafar J, Mandel G, De Lara F. Natural history of brainstem cavernous malformations. Neurosurgery 2001;48:47–53.

[28] Wiestler OD, Schiffer D, Coons SW, Prayson RA, Rosenblum MK. Ependymoma. In: Kleihues P, Cavanee WK, editors. Pathology and genetics. Tumors of the nervous system. Lyon: International Agency for Research on Cancer; 2000, p. 72–6.

[29] Burger PC, Scheithauer BW. Tumors of neuroglia and choroid plexus epithelium. In: Tumors of the central nervous system. Washington DC: Armed Forces Institute of Pathology; 1994, p. 25–161.

[30] Paulus W, Jellinger K, Morgello S, Deckert-Schlüter M. Malignant lymphomas. In: Kleihues P, Cavanee WK, editors. Pathology and genetics. Tumors of the nervous system. Lyon: International Agency for Research on Cancer; 2000, p. 198–203.

[31] Nasir S, DeAngelis LM. Update on the management of primary CNS lymphoma. Oncology (Huntingt) 2000;14:228–34.

[32] Hankey GJ, Warlow CP. The role of imaging in the management of cerebral and ocular ischemia. Neuroradiology 1991;33:381–90.

[33] Van der Zwan A, Hillen B, Tulleken CA, Dujovny M, Dragovic L. Variability of the territory of the major cerebral arteries. J Neurosurg 1992;77:927–40.

[34] Janssen O, Brückmann H, Ischämische H. In: Sartor K, editor. Neuroradiologie, 2nd ed. Stuttgart: Thieme; 2001, p. 140–58.

[35] Fauci AS, Haynes B, Katz P. NIH conference. The spectrum of vasculitis: clinical, pathologic, immunologic, and therapeutic considerations. Ann Intern Med 1978;89:660–76.

[36] Block F, Reith W. Isolierte Vaskulitis des ZNS. Radiologe 2001;40:1090–7.

[37] Ferro JM. Vasculitis of the cerebral nervous system. J Neurol 1998;245:766–76.

[38] Smirniotopoulos JG, Murphy FM. Central nervous system manifestation of the phakomatoses and other inherited syndromes. In: Atlas SW, editor. Magnetic resonance imaging of the brain and spine, 2nd ed. Philadelphia: Lippincott-Raven; 1996, p. 773–802.

[39] Van der Knaap MS, Valk J, editors. Magnetic resonance of myelitis, myelination, and myelin disorders. 2nd ed. Springer, 1995.

[40] Edwards-Brown ME, Bonin JM. White matter diseases. In: Atlas SW, editor. Magnetic resonance imaging of the brain and spine. Philadelphia: Lippincott-Raven; 1996, p. 649–706.

[41] McDonald WI, Compston A, Edan G, Goodkin D, Hartung HP, Lublin FD, McFarland HF, Paty DW, Polman CH, Reingold SG, Sandberg-Wollheim M, Sibley W, Thompson A, van den Noort S, Weinhenker BY, Wolinski JS. Recommended diagnostic criteria multiple sclerosis: guidelines from the international panel on diagnosis of multiple sclerosis. Ann Neurol 2001;50:121–7.

[42] Filippi M, Rocca MA, Wiessmann M, Mennes S, Cercignani M, Yousri TA, Soriani MP. A comparison of MR imaging with fast-FLAIR, HASTE FLAIR, and EPI-FLAIR sequences in the assessment of patients with multiple sclerosis. AJNR Am J Neuroradiol 1999;20:1931–8.

[43] Reiche W, Merkelbach S, Reith W. Neuroradiologische Aspekte bei Encephalitis disseminata. Radiologe 2000;40:1045–56.
[44] Horowitz AL, Kaplan RD, Grewe G, White RT, Salberg LM. The ovoid lesion: a new MR observation in patients with multiple sclerosis. AJNR Am J Neuroradiol 1989;10:303–5.
[45] Paty DW. MRI as a method to reveal in vivo pathology in MS. J Neural Transm [Suppl] 1997;49:211–7.
[46] Osborn A. Infections of the brain and its linings. In: Osborn A, editor. Diagnostic neuroradiology. St. Louis: Mosby; 1994b, p. 673–715.
[47] Barkovich JA. Pediatric neuroimaging, 2nd ed. Philadelphia: Lippincott-Raven, 2000.
[48] Galluci M, Bozzao A, Splendiani A, Maciocchi C, Passariello R. Wernicke encephalopathy: MR findings on eight patients. AJNR Am J Neuroradiol 1990;11:887–92.
[49] Schroth G, Wichmann W, Valavanis A. blood brain barrier disruption in acute Wernicke encephalopathy: MR findings. J Comput Assist Tomogr 1991;15:1059–60.
[50] Zajicek JP, Scolding NJ, Foster O, Rovaris M, Evanson J, Moseley IF, Scadding JW, Thompson EJ, Chamoun V, Miller DH, McDonald WI, Mitchell D. Central nervous system sarcoidosis—diagnosis and management. Q J Med 1999;92:103–17.